AGU PUBLICATIONS

Geochemistry, Geophysics, Geosystems

RESEARCH ARTICLE
10.1002/2016GC006477

Special Section:
The Arctic: An AGU Joint Special Collection

Mineralogical, geochemical, and magnetic signatures of surface sediments from the Canadian Beaufort Shelf and Amundsen Gulf (Canadian Arctic)

Adriana Gamboa[1,2,3], Jean-Carlos Montero-Serrano[1,2,4], Guillaume St-Onge[1,4,5], André Rochon[1,4], and Pierre-Arnaud Desiage[1,4,5]

[1]Institut des sciences de la mer de Rimouski, Université du Québec à Rimouski, Rimouski, Québec, Canada, [2]Postgrado en Ciencias Marinas, Instituto Oceanográfico de Venezuela, Universidad de Oriente, Cumaná, Venezuela, [3]Coordinación de Procesos Químicos, Universidad Politécnica del Oeste de Sucre "Clodosbaldo Russián", Cumaná, Venezuela, [4]GEOTOP Research Center, Montréal, Québec, Canada, [5]Canada Research Chair in Marine Geology, Institut des sciences de la mer de Rimouski, Université du Québec à Rimouski, Rimouski, Québec, Canada

Key Points:
- Tracking sediment provenance in the Canadian Beaufort Shelf and Amundsen Gulf
- Coupling grain size, mineralogical, geochemical, and magnetic proxies in the western Canadian Arctic
- Dolomite-K-feldspar and Ca-Mg characterize southwestern Banks Island
- Phyllosilicates-magnetite-Fe-oxides and Al-K-Ti-Fe-Cr-V-Zn-P characterize the Canadian Beaufort Shelf
- The Canadian Beaufort Shelf and Amundsen Gulf are separated into four sedimentological provinces

Supporting Information:
- Supporting Information S1

Correspondence to:
J.-C. Montero-Serrano,
jeancarlos_monteroserrano@uqar.ca

Citation:
Gamboa, A., J.-C. Montero-Serrano, G. St-Onge, A. Rochon, and P.-A. Desiage (2017), Mineralogical, geochemical, and magnetic signatures of surface sediments from the Canadian Beaufort Shelf and Amundsen Gulf (Canadian Arctic), *Geochem. Geophys. Geosyst.*, *18*, doi:10.1002/2016GC006477.

Received 7 JUN 2016
Accepted 28 DEC 2016
Accepted article online 3 JAN 2017

Abstract Mineralogical, geochemical, magnetic, and siliciclastic grain-size signatures of 34 surface sediment samples from the Mackenzie-Beaufort Sea Slope and Amundsen Gulf were studied in order to better constrain the redox status, detrital particle provenance, and sediment dynamics in the western Canadian Arctic. Redox-sensitive elements (Mn, Fe, V, Cr, Zn) indicate that modern sedimentary deposition within the Mackenzie-Beaufort Sea Slope and Amundsen Gulf took place under oxic bottom-water conditions, with more turbulent mixing conditions and thus a well-oxygenated water column prevailing within the Amundsen Gulf. The analytical data obtained, combined with multivariate statistical (notably, principal component and fuzzy c-means clustering analyses) and spatial analyses, allowed the division of the study area into four provinces with distinct sedimentary compositions: (1) the Mackenzie Trough-Canadian Beaufort Shelf with high phyllosilicate-Fe oxide-magnetite and Al-K-Ti-Fe-Cr-V-Zn-P contents; (2) Southwestern Banks Island, characterized by high dolomite-K-feldspar and Ca-Mg-LOI contents; (3) the Central Amundsen Gulf, a transitional zone typified by intermediate phyllosilicate-magnetite-K-feldspar-dolomite and Al-K-Ti-Fe-Mn-V-Zn-Sr-Ca-Mg-LOI contents; and (4) mud volcanoes on the Canadian Beaufort Shelf distinguished by poorly sorted coarse-silt with high quartz-plagioclase-authigenic carbonate and Si-Zr contents, as well as high magnetic susceptibility. Our results also confirm that the present-day sedimentary dynamics on the Canadian Beaufort Shelf is mainly controlled by sediment supply from the Mackenzie River. Overall, these insights provide a basis for future studies using mineralogical, geochemical, and magnetic signatures of Canadian Arctic sediments in order to reconstruct past variations in sediment inputs and transport pathways related to late Quaternary climate and oceanographic changes.

1. Introduction

Sedimentation in the Arctic Ocean is characterized by high terrigenous input from the surrounding continents with different petrographic signatures [*Harrison et al*., 2011]. These sediments are delivered into the Arctic Ocean mainly as suspended particulate matter and bed loads from several large river systems (notably, the Mackenzie, Kolyma, Lena, Ob, Yenisei, Pechora, and Severnaya Dvina) [*Holmes et al*., 2002; *Wagner et al*., 2011] and from coastal erosion, and then dispersed by ocean currents (summarized in *Stein* [2008]). Furthermore, in shallow margins, suspended terrigenous particles can also be incorporated in sea ice during its formation and then be transported via ocean currents over long distances throughout the Arctic Ocean, to finally settle far from their source of origin [e.g., *Bischof et al*., 1996; *Darby et al*., 2012, 2006].

Taking this into account, a number of studies have characterized the mineralogical and geochemical composition of the detrital sediments over the continental shelf from the Eurasian Basin [e.g., *Vogt*, 1997; *Schoster et al*., 2000; *Viscosi-Shirley et al*., 2003; *Stein*, 2008; *Bazhenova*, 2012], Chukchi Sea-Bering Strait [e.g., *Asahara et al*., 2012; *Linsen et al*., 2014], and Chukchi-Alaskan margin [e.g., *Naidu et al*., 1982; *Naidu and Mowatt*, 1983; *Ortiz et al*., 2009; *Darby et al*., 2012] to decipher: (1) variations in detrital particle provenance, (2) climate and atmospheric circulation changes in the source areas on adjacent landmasses, and (3)

changes in sediment propagation and ocean-current pathways. However, few studies provide a general view of the surface detrital provenances and sediment-dispersal patterns within the Mackenzie-Beaufort Sea Slope and Amundsen Gulf [e.g., *Naidu et al*., 1971; *Bornhold*, 1975; *Pelletier*, 1975; *Davidson et al*., 1988; *Hill et al*., 1991; *Darby et al*., 2011; *Vonk et al*., 2015] compared to other Arctic continental shelf regions. To our knowledge, no general mineralogical and geochemical distributions of the Canadian Beaufort Shelf and Amundsen Gulf are available today. Such studies may provide a baseline to better interpret, in terms of sediment dynamics and climate change, the mineralogical and geochemical signatures preserved in the southern Beaufort Sea sedimentary records, which may then help to place current western Arctic climate change [e.g., *Kwok et al*., 2009] into its broader context.

In this study, a multiproxy analysis was carried out on the bulk detrital fraction of surface sediment samples from the Mackenzie-Beaufort Sea Slope and Amundsen Gulf in order to: (1) characterize the spatial distribution patterns of siliciclastic grain size, magnetic properties, bulk minerals, and elemental geochemistry in surface sediments; (2) identify different sedimentary provinces, source areas, and transport pathways of terrigenous material; and (3) better constrain modern sediment dynamics within the western Canadian Arctic. Overall, this study provides a unique opportunity to compare mineralogical, geochemical, magnetic, and siliciclastic grain-size signatures within the Mackenzie-Beaufort Sea Slope and Amundsen Gulf area.

2. Environmental Setting

2.1. Regional Morphology

The Canadian Beaufort Shelf is a shallow platform located along the northwestern Canadian coast in the southeastern Beaufort Sea (western Arctic Ocean; Figure 1). It is bordered to the west by the Mackenzie Trough and to the east by the Amundsen Gulf. This shelf is cut by several partially infilled cross-shelf channels: the Ikit Trough, the Kugmallit Channel, and the Niglik Channel [*Blasco et al*., 2013]. Moreover, several hundreds of conical mounds, locally referred to as pingo-like-features [*Shearer et al*., 1971], occur across the Canadian Beaufort Shelf [*Blasco et al*., 2013]. Based on seismic reflection profiles, water column acoustic anomalies [*Paull et al*., 2007; *Blasco et al*., 2013; *Saint-Ange et al*., 2014; *Paull et al*., 2015] together with geochemical composition of pore waters, gas and sediments [*Paull et al*., 2015], these conical features are now regarded as mud volcanoes. On the other hand, the Amundsen Gulf is a large channel (400 km-long, 200 km-wide, average water depth of 300 m) [*Stokes et al*., 2006] that connects the southeastern Beaufort Sea to the Canadian Arctic Archipelago (Figure 1). It is bordered by the Banks Island Shelf to the north and by the Mackenzie Shelf to the southwest.

The Canadian Beaufort Shelf and Amundsen Gulf are nearly completely covered by sea ice (pack-ice and landfast ice) from September/October to May [*Barber and Hanesiak*, 2004; *Galley et al*., 2008], with great annual and interannual variability [e.g., *Schell et al*., 2008; *Bringué and Rochon*, 2012]. In summer, freshet from the Mackenzie River, wind forcing, and rising air temperatures result in ice-free conditions over the shelf by late July and over the slope in August [*O'Brien et al*., 2006]. In addition, in the middle of landfast ice from the Amundsen Gulf, the ice-free zone forms part of the Cape Bathurst Polynya which develops during winter at approximately the same location under the action of winds, currents and upwellings of warmer water [*Arrigo and van Dijken*, 2004]. In this ice-free area, stronger westerly to northwesterly winds induce turbulent mixing of the water column [e.g., *Magen*, 2007; *Forest et al*., 2008; *Tremblay et al*., 2014].

2.2. Surrounding Geology

The Mackenzie River drainage basin covers a large part of western Canada ($\sim 1.8 \times 10^6$ km^2) [*Carson et al*., 1998; *Hill et al*., 2001]. Three main geological units characterize the Mackenzie River basin [*Millot et al*., 2003]: (1) the North American Cordillera (including the Rocky and the Mackenzie Mountains) in the western part, distinguished by volcanic and immature volcano-clastic sediments in the western Canadian orogenic belt (Stikine terrane) and carbonates and slates in the Mackenzie Mountains; (2) the Interior Platform (lowlands), composed of marine and non-marine sedimentary rocks (Cambrian to Cretaceous limestones, shales, and sandstones); and (3) the Canadian Shield in the eastern part, typified by old silicate rocks (Archean granites and gneisses) from the Slave Province [*Padgham and Fyson*, 1992]. In turn, Banks Island is composed of Cretaceous shale and sandstone, Upper Devonian sandstone and shale, and Tertiary-Quaternary glacial deposits, which are rich in dolomite clasts as well as quartz and feldspar grains [*Bischof et al*., 1996; *Bischof and Darby*, 1999].

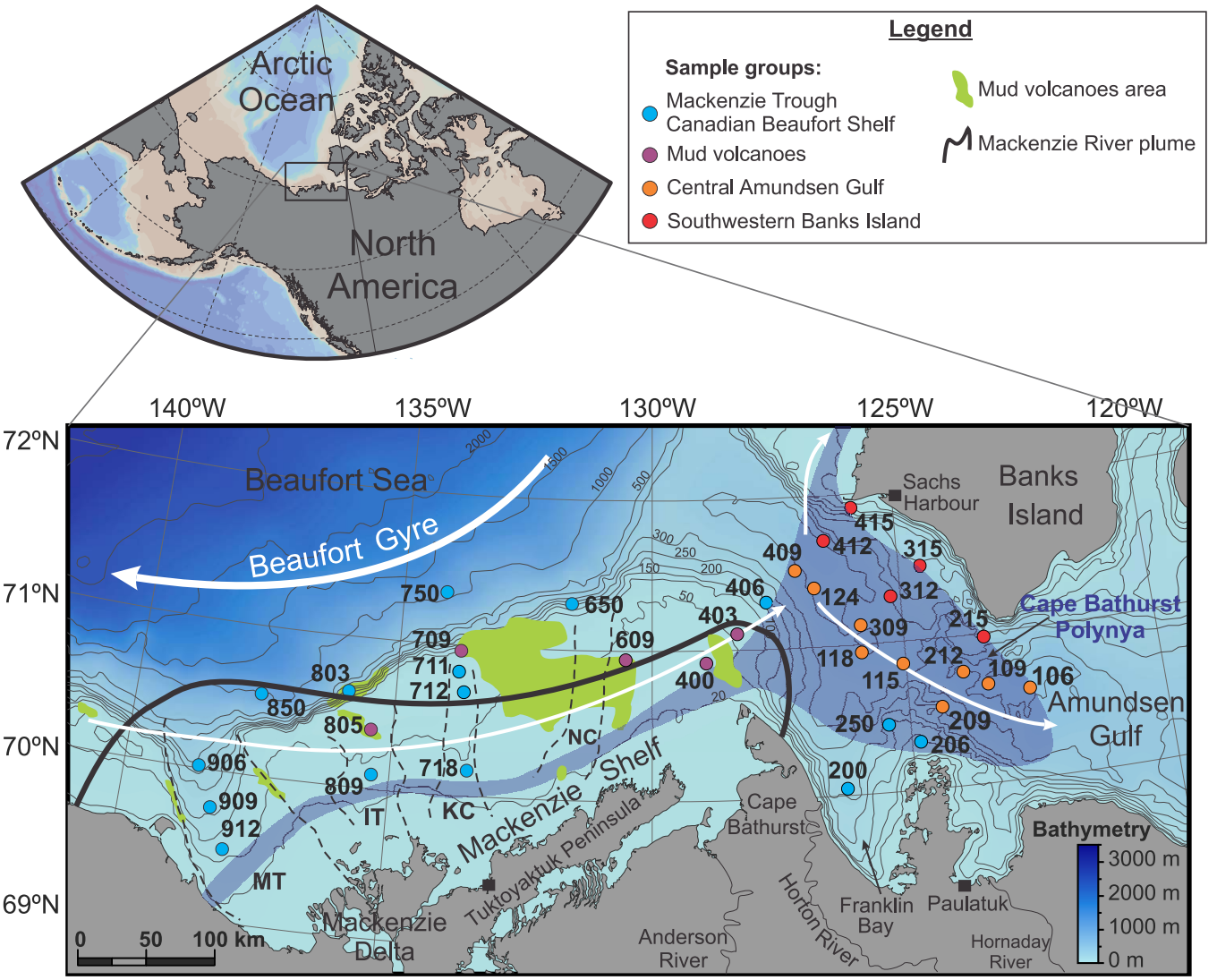

Figure 1. Map of the Beaufort Sea and Amundsen Gulf illustrating the location of surface sediment samples used in this study. Partially infilled cross-shelf channels (IT: Ikit Trough, KC: Kugmallit Channel, NC: Niglik Channel) and distribution of mud volcanoes across the Beaufort Shelf are also illustrated [*Blasco et al.*, 2013]. MT represents the Mackenzie Trough; the thick white arrows represent the coastal surface circulation which is dominated by the Beaufort Undercurrent (here represented under westerly influence); the black line indicates the maximum extent of the Mackenzie River Plume; and the light blue shading represents the extent of the spring ice-free zone.

2.3. Sedimentation

The Mackenzie River is the fourth-largest (after the Yenisei, Lena, and Ob rivers) Arctic river in terms of freshwater discharge (~420 km^3/yr) [*Wagner et al.*, 2011], but the first in terms of sediment discharge (~127 Mt/yr) [*Carson et al.*, 1998]. This large suspended sediment discharge of the Mackenzie River forms a large sediment plume (generally 2–3 m thick) [*Hill et al.*, 1991] on the Canadian Beaufort Shelf (Figure 1). The transport of suspended sediments within this plume is affected by the ice cover, winds, and currents [*Carmack and Macdonald*, 2002]. In winter, the Mackenzie River discharges are trapped on the inner shelf by the stamukhi (a field of ice fragments), which acts as an inverted dam and causes the formation of the "floating freshwater" lake Herlinveaux [*Macdonald et al.*, 1995]. In summer, the plume's position is greatly affected by prevailing winds, with winds from the northwest pushing the plume along Tuktoyaktuk Peninsula [*Giovando and Herlinveaux*, 1981], and winds from the southeast pushing the plume westward, beyond the Mackenzie Trough [*MacNeil and Garrett*, 1975]. In addition, although coastal erosion is an important local sediment supply near the shoreline, its estimated contribution (~7 Mt/yr) is dwarfed by that of the Mackenzie River [*Carmack and Macdonald*, 2002]. Furthermore, the suspended particulate matter supply to the Amundsen Gulf is much smaller than to the Canadian Beaufort shelf as no large rivers discharge into the Gulf

[*Macdonald et al*., 1998]. Indeed, small rivers located to the east of the Mackenzie River, such as the Anderson, Horton and Hornaday Rivers (Figure 1), have a weak mean annual freshwater discharge (<146 m^3/s; R-ArcticNet database: http://www.r-arcticnet.sr.unh.edu/v4.0/index.html) [*Lammers et al*., 2001], and therefore, contribute weakly to the sedimentation in the eastern Mackenzie Shelf and Amundsen Gulf. Consequently, modern sedimentation rates are high within the Mackenzie Trough (~40–320 cm/ka) *Macdonald et al*., 1998; *Richerol et al*., 2008a; *Durantou et al*., 2012] and on the nearby continental shelf and slope (~100–200 cm/ka) [*Barletta et al*., 2008; *Scott et al*., 2009; *Bringué and Rochon*, 2012]. To the east, these modern sedimentation rates decrease toward Amundsen Gulf (<80 cm/ka) [*Macdonald et al*., 1998; *Schell et al*., 2008], where sediment hardly accumulates at all [*Hill et al*., 1991].

On the Canadian Beaufort shelf, most of the surficial seabed sediments are predominantly composed of Holocene marine olive-grey silts and clays [e.g., *Pelletier*, 1975; *Hill et al*., 1991; *Barletta et al*., 2008; *Scott et al*., 2009]. Surface sediments from the Amundsen Gulf are composed of a relatively thin layer of olive-grey silty clay overlying a diamicton of brownish red color with abundant pebbles and cobbles [*Bennett et al*., 2008; *Schell et al*., 2008; *Scott et al*., 2009].

2.4. Oceanic Circulation

Oceanic circulation in the southeastern Beaufort Sea is dominated by the anticyclonic Beaufort Gyre (BG), which pushes both surface currents and sea-ice westward at the shelf break (Figure 1). Conversely, closer to shore around the 50 m isobath, the Beaufort Undercurrent transports both Pacific and Atlantic waters eastwards along the continental margin and into Amundsen Gulf [e.g., *Aagaard*, 1984; *Pickart*, 2004; *Bringué and Rochon*, 2012; *Durantou et al*., 2012]. In general, surface waters influenced by the anticyclonic BG enter Amundsen Gulf near southwestern Banks Island and exit near Cape Bathurst [*Lanos*, 2009]. At a regional level, these surface circulation regimes are mainly controlled by changes in the phase of large-scale atmospheric patterns such as the Arctic Oscillation (AO) [*Darby et al*., 2001; *Macdonald et al*., 2005] and the Pacific Decadal Oscillation (PDO) [*Overland et al*., 1999; *Durantou et al*., 2012], which are both significant natural patterns in global climate variability.

3. Material and Methods

3.1. Samples

A total of 34 surface sediment samples were collected at different depths in the Canadian Beaufort Shelf and Amundsen Gulf on board the Canadian Coast Guard Ship (CCGS) Amundsen during the CASES (Canadian Arctic Shelf Exchange Study) 2004 expedition (Rochon and onboard participants, 2004). The sampling was performed using a box core sampler (0.5 m × 0.5 m × 0.5 m) wherein the uppermost 5 mm of sediment was recovered in order to collect only the sediment-water interface [*Richerol et al*., 2008b]. Based on the regional morphology, mud volcanoes distribution [*Blasco et al*., 2013], and the influence of the Mackenzie River plume [*Richerol et al*., 2008b; *Scott et al*., 2008], the surface sediment samples were divided into four main geographical areas (Figure 1): (1) Mackenzie Trough-Canadian Beaufort Shelf, (2) mud volcanoes, (3) central Amundsen Gulf, and (4) southwestern Banks Island.

3.2. Analytical Procedure

3.2.1. Grain-Size Distribution

Sediment grain-size analyses were performed on the detrital fraction of the sediment using a Beckman Coulter LS13320 laser diffraction grain-size analyzer, which has a detection range of 0.04–2000 μm. Samples were deflocculated by successive washing with distilled water after the removal of organic matter and biogenic carbonate of the sediments with 10 mL of hydrogen peroxide (30% H_2O_2) and 10 mL of hydrochloric acid (0.5 *M* HCl), respectively. Biogenic silica was not removed as it appeared to be negligible (likely less than 1%, as suggested by its non detection in the bulk sediment XRD diffractograms). The grain-size distribution and statistical parameters (e.g., mean, sorting) were calculated using the moment methods in logarithmic (phi—ϕ) scale and the GRADISTAT software [*Blott and Pye*, 2001]. Furthermore, the end-member modelling algorithm (EMMA) developed by *Weltje* [1997] and adapted by *Dietze et al*. [2012] was subsequently applied to the grain-size data in order to extract meaningful end-member (EM) grain-size distributions and estimate their proportional contribution to the sediments. The cumulative explained variance (r^2) was calculated to assess the minimum number of EMs needed for a good estimate of our grain-size data

[*Weltje*, 1997; *Dietze et al*., 2012]. In general, grain-size distribution and end-member modelling analysis can be used to investigate the sedimentary transfer regime because sediment grain-size distribution (primarily driven by sedimentary processes) reflects transport conditions [e.g., *Montero-Serrano et al*., 2009, 2010a; *Simon et al*., 2012; *Dietze et al*., 2012].

3.2.2. Bulk Magnetic Properties

Low-field magnetic susceptibility (k_{lf}) was measured on bulk sediment samples using a Bartington MS2E. The k_{lf} values primarily reflect changes in the ferrimagnetic concentration (e.g., magnetite or titanomagnetite), but they are also sensitive to magnetic grain-size variations [*Dunlop and Özdemir*, 1997]. In order to explore the possible presence of superparamagnetic particles, magnetic susceptibility was measured in some bulk sediment samples, at low (0.465 kHz; k_{lf}) and high (4.65 kHz; k_{hf}) frequencies on a Bartington Susceptibility Meter (model MS2B) with a dual-frequency sensor. The sample measuring time was 10 s. Each measurement was repeated five times and the readings were averaged. The measurement of hysteresis loops and derived properties, including saturation remanence (M_r), saturation magnetization (M_s), bulk coercive force (H_c), and remanent coercive force (H_{cr}) were determined using an alternating gradient force magnetometer (AGM) MicroMag 2900 from Princeton Measurements Corporation. The M_{rs}/M_s and H_{cr}/H_c ratios can be used as grain-size proxies (the so-called Day plot) as well as to identify the magnetic domain state when the principal remanence-carrier mineral is magnetite [*Day et al*., 1977; *Dunlop*, 2002; *Stoner and St-Onge*, 2007].

3.2.3. Bulk Sediment Mineralogy and Elemental Geochemistry

Before the bulk mineralogical and geochemical analysis, the sediment samples were rinsed five times with distilled water after the removal of organic matter fraction with 10 mL of hydrogen peroxide (30% H_2O_2). Next, sediment samples were ground with a McCrone micronizing mill using 5 mL of ethanol and grinding times of 5–10 min to obtain a homogeneous powder. The slurry was oven-dried oven-dried at about 60°C and then slightly homogenized with an agate mortar to prevent any agglomeration of finer particles during drying. Aliquots of these sediment samples were used for bulk mineralogical and geochemical analysis.

Bulk mineral associations were studied by X-ray diffraction (XRD). The random powder samples were side-loaded into the holders and analyzed on a PANalytical X'Pert Powder diffractometer. This instrument is fitted with a copper tube (Cu K-alpha = 1.54178 Å), operating at 45 kV and 40 mA and a postdiffraction graphite monochromator. Samples were scanned from 5° to 65° two-theta in steps of 0.020° two-theta and a counting time of 2 s per step. For the semiquantification of the major mineralogical components, bulk sediment XRD scans were processed in the software package X'Pert High-Score Plus (PANalytical) using the Rietveld full-pattern fitting method [e.g., *Young*, 1993; *Grunsky et al*., 2013]. This method permits the semiquantification of whole-sediment mineralogy with a precision of 5–10% for phyllosilicates and 5% for nonphyllosilicate minerals. The quality of the Rietveld fitting procedure was evaluated for the R-profile and goodness-of-fit (GOF). The R-profile quantifies the difference between the observed and calculated patterns, whereas the GOF is the ratio between the R-weighted profile (RWP; best least-square fit between observed and calculated patterns) and R-expected theoretical (Rexp; best possible value for the residual). An R-value profile between 20–30% and a GOF of fewer than 3 are typically adequate in the Rietveld refinement of geological samples [e.g., *Young*, 1993]. The major mineralogical components quantified by this technique are: quartz, potassium feldspar (microcline + orthoclase), plagioclase feldspar (albite + anorthite), amphibole (hornblende), pyroxene (augite), magnetite, Fe-oxides (hematite + goethite), dolomite, and phyllosilicates (biotite, muscovite, illite, chlorite, and kaolinite).

A total of 14 elements (Al, Si, K, Mg, Ca, Ti, Mn, Fe, P, Sr, V, Cr, Zn, and Zr) were analyzed by energy dispersive X-ray fluorescence (EDXRF) spectrometry using a PANalytical Epsilon 3-XL. Before EDXRF analysis, loss on ignition (LOI) was determined gravimetrically by heating the dried samples up to 950°C for 2 h. Subsequently, samples were treated by borate fusion in an automated fusion furnace (CLAISSE® M4 Fluxer). Samples weighing ~0.6 g were mixed with ~6 g of lithium borate flux (CLAISSE, pure, 49.75% $Li_2B_4O_7$, 49.75% $LiBO_2$, 0.5% LiBr). The mixtures were melted in Pt-Au crucibles (95% Pt, 5% Au), and after fusion, the melts were cast to flat disks (diameter: 32 mm; height: 3 mm) in Pt-Au moulds. Acquired XRF spectra were processed with the standardless Omnian software package (PANalytical). The resulting data are expressed as weight percent (wt.%; Al, Si, K, Mg, Ca, Ti, Mn, Fe, P) and micrograms per gram (μg/g; V, Cr,Zn, Sr, Zr). Procedural blanks always accounted for less than 1% of the lowest concentration measured in the sediment samples. Analytical accuracy and precision were found to be better than 1–5% for major elements and 5–10% for the other elements, as checked by an international standard (USGS SDC-1) and analysis of replicate samples.

Because Al and Si are associated to clay minerals, aluminosilicates and quartz, and Ca is associated to carbonates, the ternary plot Al-Si-Ca (expressed as oxides) was used here in order to obtain a general geochemical classification of the sediments [e.g., *Brumsack*, 1989; *Meinhardt et al*., 2014]. In addition, to compare the relative enrichment of redox-sensitive elements (Mn, Fe, V, Cr, Zn), we calculated enrichment factors (EF) by comparing Al-normalized metal concentrations to those of average shale [*Wedepohl*, 1991]: $X_{EF} = [(X/Al)_{sample}/(X/Al)_{average\ shale}]$. In practical terms, $EF > 3$ represents a detectable authigenic enrichment of an element over average shale concentrations, whereas $EF > 10$ represents a moderate to strong degree of authigenic enrichment [e.g., *Tribovillard et al*., 2006].

In addition, in order to identify the presence of authigenic minerals (such as carbonate, iron oxides, and greigite) within the mud volcanoes province, some bulk sediments and white crusts observed in the samples were analyzed using a JEOL 6460LV scanning electron microscope equipped with an Energy Dispersive X-ray Spectrometer (SEM-EDS). The image and EDS analyses were obtained with a backscatter detector, an accelerating voltage of 20 kV and a spot size of 60 (probe diameter).

3.3. Statistical and Spatial Approach

The mineralogical and geochemical data are of a compositional nature, that is, they are vectors of nonnegative values subjected to a constant-sum constraint (usually 100%). This implies that relevant information is contained in the relative magnitudes, so statistical analysis must focus on the ratios between components [*Aitchison*, 1986]. Under this framework, a principal component analysis (PCA) was performed on the mineralogical and elemental geochemical data sets with the goal of finding elemental and mineralogical associations with similar relative variation patterns that may be interpreted from a palaeoenvironmental standpoint [e.g., von *Eynatten et al*., 2003; *Montero-Serrano et al*., 2010b; von *Eynatten et al*., 2016]. Likewise, a fuzzy c-means clustering analysis was performed using the mineralogical data set with the goal of ascertaining whether the differences observed between each sedimentological provinces are statistically valid. The results from the fuzzy c-means clustering are visualized by a silhouette plot [*Kaufman and Rousseeuw*, 2009], where each sediment sample is represented by a bar (silhouette width) that ranges from 0 (no similarity) to 1 (identical). Thus, the silhouette plot allows a visualization of the quality of the clustering and the distinctiveness of the sediment samples [*Borcard et al*., 2011]. Prior to all multivariate analyses, a log-centered (clr) transform was applied to the data [*Aitchison*, 1990]. The clr transform is derived by dividing each variable (e.g., mineral percentage, element concentration) by the geometric mean of the composition of the individual observations and then taking the logarithm. This operation removes statistical constraints on compositional variables, such as the constant-unit sum, and allows the valid application of classical (Euclidean) statistical methods to compositional data [*Aitchison*, 1986, 1990]. All statistical calculations were conducted with the "R" software using the packages "StatDA" [*Reimann et al*., 2008], "compositions" [van den *Boogaart and Tolosana-Delgado*, 2008], "vegan" [*Oksanen et al*., 2015], and "cluster" [*Maechler et al*., 2015]. Finally, the scores from the first two principal components of the log-centered data were used to produce interpolated compositional maps in the ArcGIS® software. The interpolated maps were generated using the Spline with Barriers algorithms available in ArcGIS®. This method of interpolation produced a smooth surface with values in the range of the scores of data points using a minimum curvature spline technique [*Childs*, 2004]. However, the interpolated surfaces closest to the borders are biased by this method and should be interpreted with caution.

4. Results and Interpretations

4.1. Grain-Size Distribution

The mean sediment grain size (phi scale) ranges from 8.31 (clay) to 6.79 (fine silts), with minimum phi values within the southwestern Banks Island province (Figure 2a). Interestingly, although all sediment samples are poorly sorted (values of $1.25 < \sigma_\phi < 1.75$; Figure 2b) in the study area, relatively higher sorting (values up to 1.75) is found in some samples from the mud volcanoes area in the Canadian Beaufort Shelf (samples 403, 609, 709, 805) as well as in the southwestern Banks Island (samples 215 and 415) (Figure 2b). In correspondence with this result, the end-member modelling analysis (EMMA) produced a three-EM model to explain more than 91% of the total variance (Figure 3a). The sediment samples are characterized by three grain classes with different grain-size distribution (Figures 3b and 3c): (1) the EM1 end-member (mean $\sim$8.8 ϕ; bimodal distribution) is associated to the clay to very fine silt fraction and characterizes many samples in

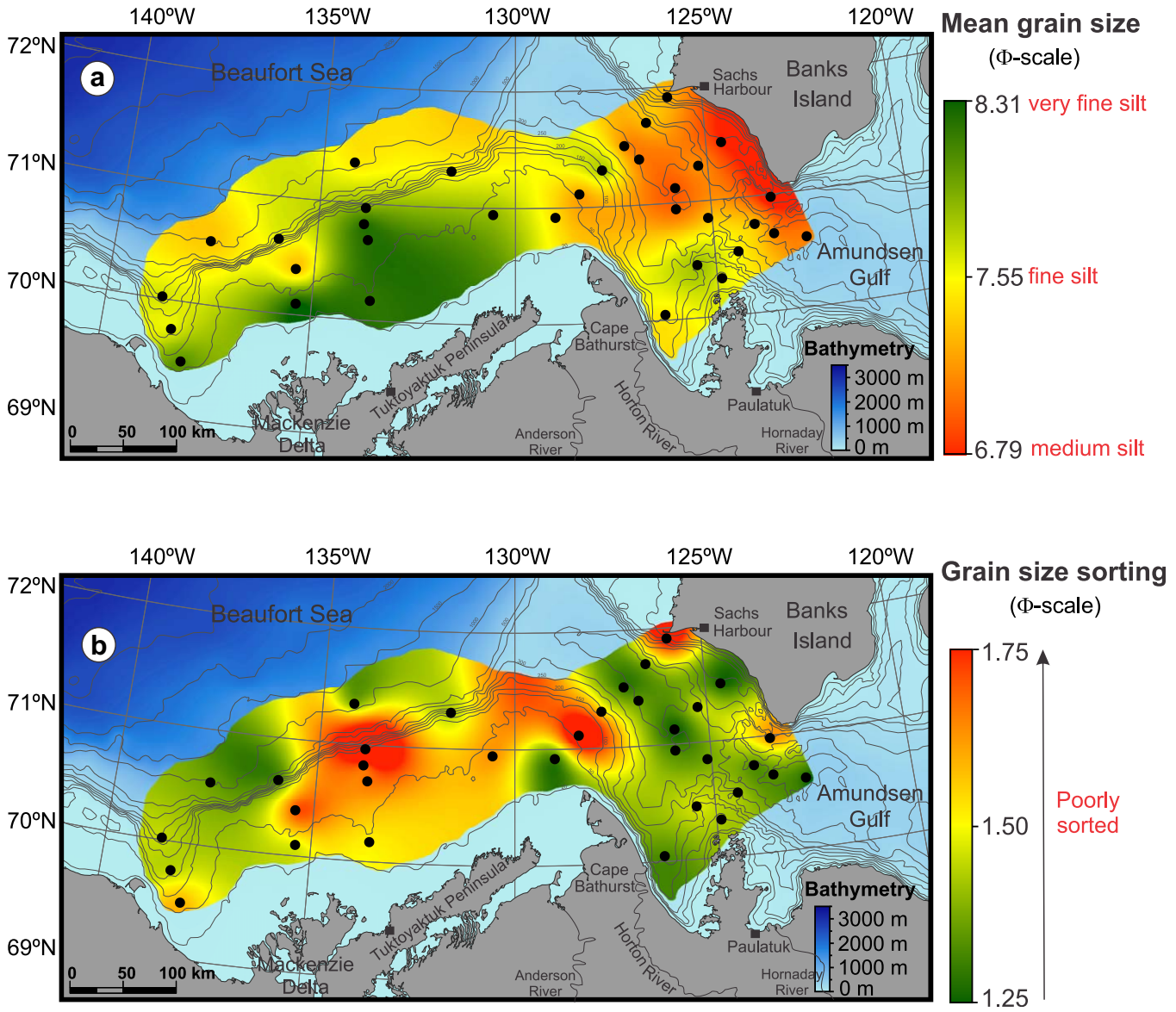

Figure 2. (a) Mean grain-size and (b) sorting distributions (phi units) for the Mackenzie-Beaufort Sea Slope and Amundsen Gulf sediments. Note that in Figure 2b, all sediment samples are poorly sorted, however, relatively higher sorting (values up to 1.75) is found in some samples from the mud volcanoes area, in the Canadian Beaufort Shelf as well as in the southwestern Banks Island.

the shallow Canadian Beaufort Shelf; (2) the EM2 end-member (mean $\sim$ 6.3 ϕ; bimodal distribution) is associated to the fine silt fraction, which is most of the sediments studied; and (3) the EM3 end-members (mean $\sim$5.9 ϕ; trimodal distribution) correspond to the medium to fine silt fraction of samples 403, 805, and 709 from the mud volcanoes in the Canadian Beaufort Shelf and 415, 312, and 315 from the southwestern Banks Island.

4.2. Magnetic Properties

Hysteresis loops of representative samples are shown in Figure 4a. All hysteresis loops display saturation fields (<250 mT) and shapes suggesting the assemblage of magnetic grains is mainly dominated by magnetite. Similarly, the $M_{rs}/M_s - H_{cr}/H_c$ cross-plots or Day plot (Figure 4b) illustrate that most of the magnetic grains within the sediment samples are composed of pseudo-single domain (PSD) magnetite [*Dunlop*, 2002]. However, some poorly sorted and coarser samples (106 and 109 from the central Amundsen Gulf; 609 and 709 from the mud volcanoes in the Canadian Beaufort Shelf; Figure 3b) show a scattered distribution on the Day plot (Figure 4b), most probably reflecting the presence of coarser magnetite grains [e.g.,

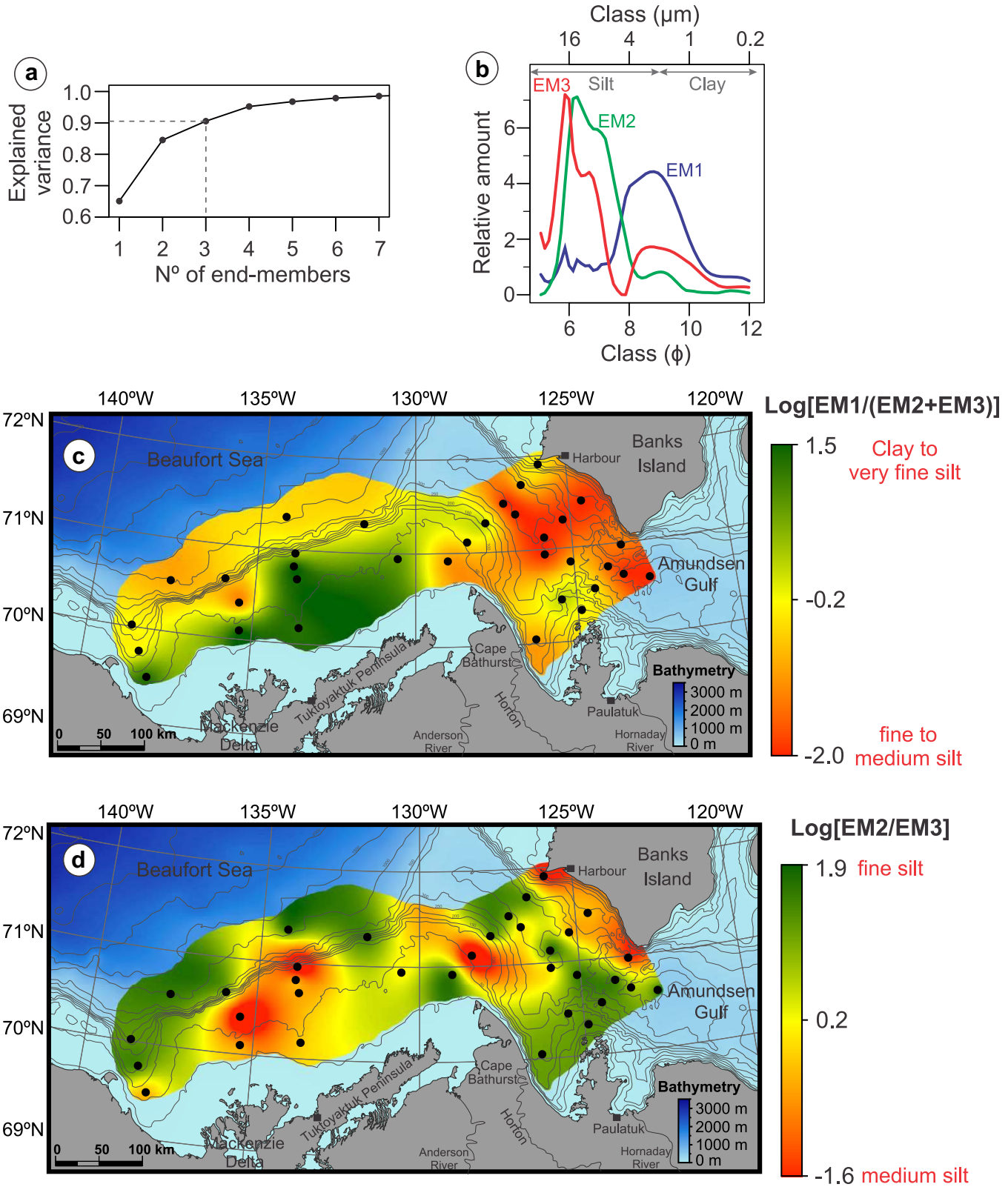

Figure 3. End-member modeling analyses (EMMA) performed on the grain-size distribution of the detrital fraction from the Canadian Beaufort Shelf and Amundsen Gulf. (a) The grain-size distribution of the first three end-members accounts for more than 91% of the total variance. (b) Three representative unmixed grain-size distributions derived from EMMA. (c) Log(EM1/EM2+EM3) and (d) Log(EM2/EM3) end-member ratios, which represent the relative proportion between clay/silts and medium-silt/coarse-silt, respectively.

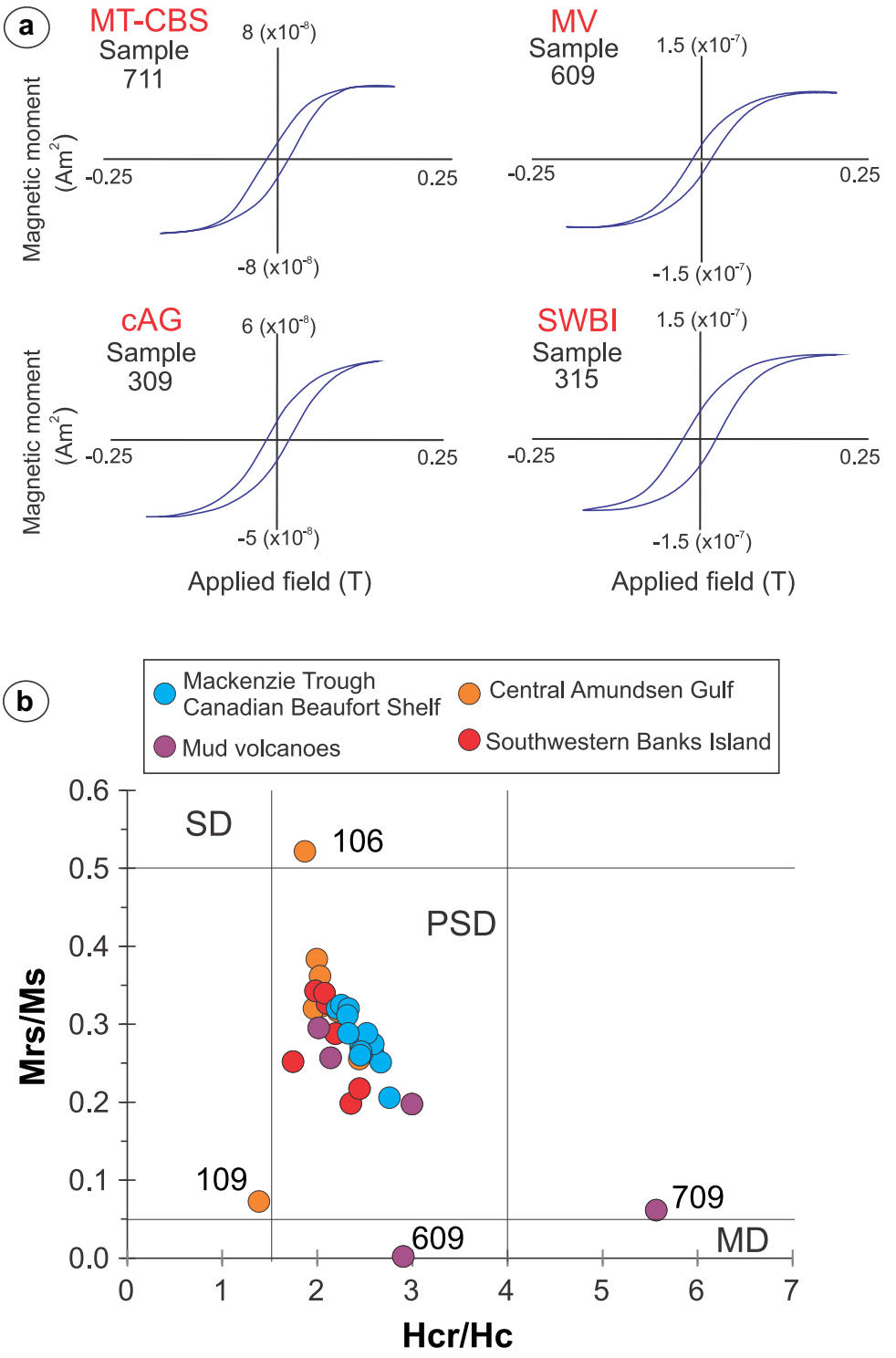

Figure 4. (a) Hysteresis loop curves for three representative samples from the Mackenzie Trough-Canadian Beaufort Shelf (MT-CBS), central Amundsen Gulf (cAG), and southwestern Banks Island (SWBI); and (b) Mrs/Ms and Hcr/Hc cross-plot (Day plot) illustrating the magnetic grain size SD (single domain), PSD (pseudo-single domain), and MD (multidomain) zonation (adapted from Day, 1977).

Lisé-Pronovost et al., 2009; *Brachfeld et al.*, 2009]. Magnetic susceptibility values range between 4.4 and 35.7 ($\times 10^{-5}$ SI units; Figure 5a), with maximum values recorded in samples from the southwestern Banks Island coast (samples 215 and 415), central Amundsen Gulf (sample 115) and mud volcanoes in the Canadian Beaufort Shelf (samples 400, 403, 609, 709, and 803). Differences in the frequency-dependent susceptibility

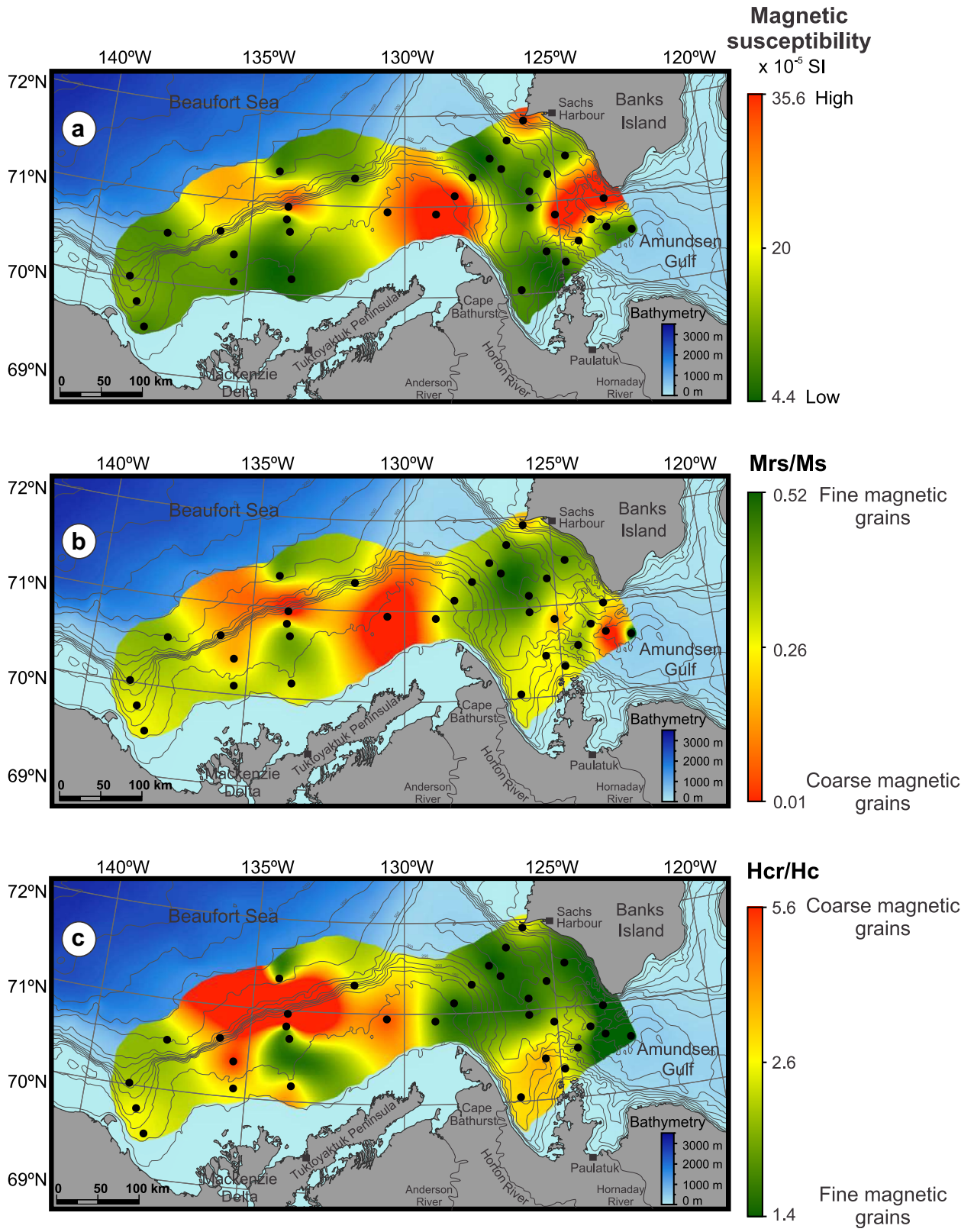

Figure 5. Magnetic properties of surface sediments from the Canadian Beaufort Shelf and Amundsen Gulf. (a) Spatial distribution of magnetic susceptibility (k_{lf}); (b) Spatial distribution of Mrs/Ms ratio; (c) Spatial distribution of Hcr/Hc ratio. Note that all magnetic parameters show similar spatial distributions.

for these last sediment samples are negligible ($k_{lf}/k_{hf} \sim 1$; supporting information Table S1), suggesting low to very low contents of superparamagnetic grains. The magnetic susceptibility, M_{rs}/M_s and H_{cr}/H_c ratios show similar distribution patterns (Figure 5), most likely suggesting that magnetic susceptibility changes are driven by magnetic grain-size variations. Interestingly, the southwestern Banks Island coast and Amundsen Gulf grains have slightly lower ratios of H_{cr}/H_c and higher ratios of M_{rs}/M_s than the Mackenzie Trough-Canadian Beaufort Shelf samples (Figures 5b, 5C and 12f), possibly indicating a slighter finer magnetic grain size. Similar results in magnetic mineralogy have also been reported in the sedimentary records from the Mackenzie Trough-Canadian Beaufort Shelf area [e.g., *Barletta et al*., 2010; *Barris*, 2012].

4.3. Bulk Mineralogy Composition

The Mackenzie Trough-Canadian Beaufort Shelf and Amundsen Gulf bulk mineralogy (supporting information Figure S1) is dominated by quartz (28–64%), phyllosilicates (15–48%), dolomite (3–35%), Na-plagioclase (4–11%), and K-feldspar (3–10%), and by lower proportions of Fe-oxides (0.2–1.5%), calcite (<1%), magnetite (<0.7%), and pyroxene (<1.0%). Amorphous silica (e.g., diatoms) was not detected in the XRD diffractograms in the studied samples due to its low content (likely <1%). Quartz, K-feldspar, plagioclase, phyllosilicates, and dolomite represented more than 91% of the overall mineral concentration in the sediment samples. In order to reduce dimensionality in the data and identify mineral associations, a principal component analysis (PCA) was conducted (Figure 6a). This analysis indicates that PC-1 (65.37% of the total variance) is positively associated with dolomite and negatively associated with phyllosilicates, Fe-oxides, and magnetite, whereas PC-2 (19.54% of the total variance) is positively associated with plagioclase and quartz and negatively associated with K-feldspar as well as dolomite, magnetite, and Fe-oxides (Figure 6b). The spatial distributions of the PC-1 and PC-2 mineralogical scores (Figure 7) reveal that the southwestern Banks Island and central Amundsen Gulf provinces are relatively enriched in dolomite and K-feldspar, whereas the Mackenzie Trough-Canadian Beaufort Shelf is characterized by higher contents in phyllosilicates, Fe-oxides, and magnetite (Figure 7a). Intermediate PC-1 scores and high PC-2 scores (up to 1.4) are observed in the coarse multimodal samples from the mud volcano province and reflect intermediate and higher concentrations of dolomite and plagioclase-quartz, respectively (Figure 7b).

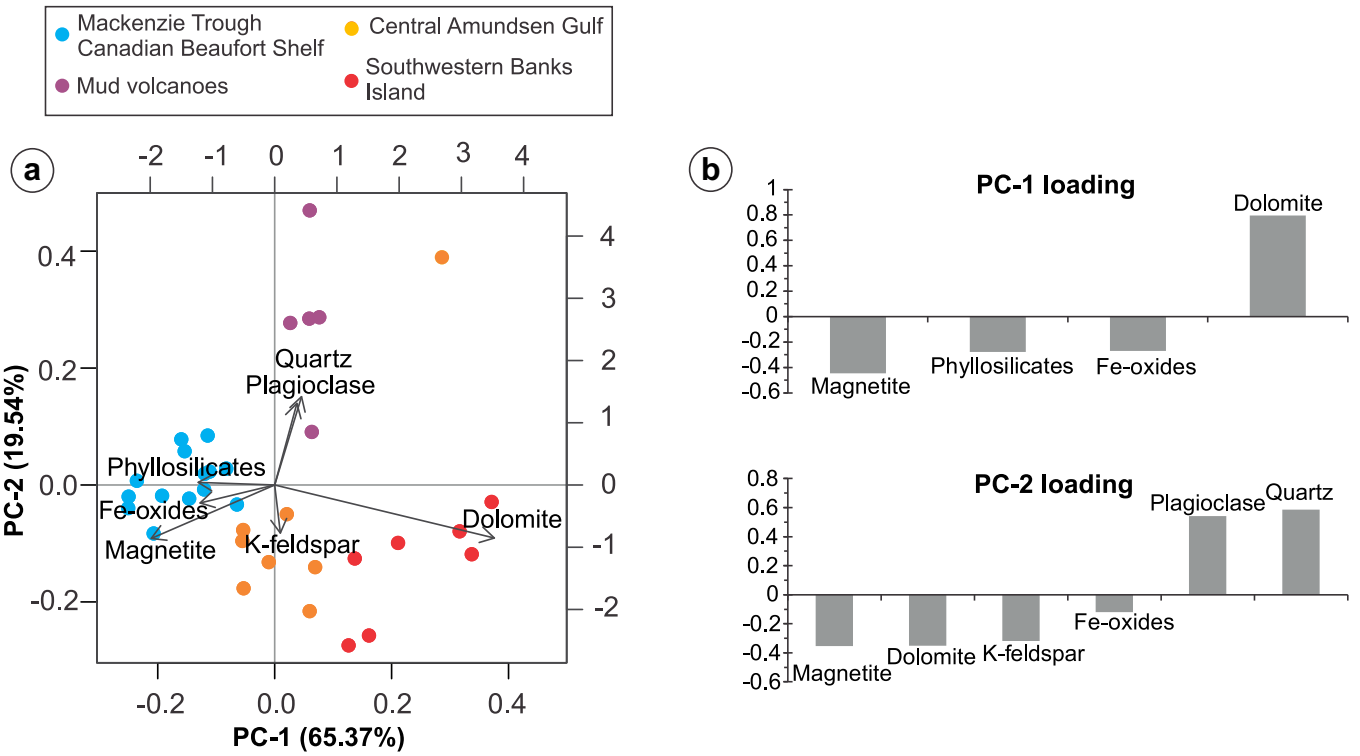

Figure 6. (a) Biplot of the PC-1 versus PC-2 obtained from the log-centered transformation of the bulk mineralogical data from the Canadian Beaufort Shelf and Amundsen Gulf sediments. (b) Loadings derived from the principal component analysis illustrating the weight (>0.1) of each mineral in the definition of each PC score.

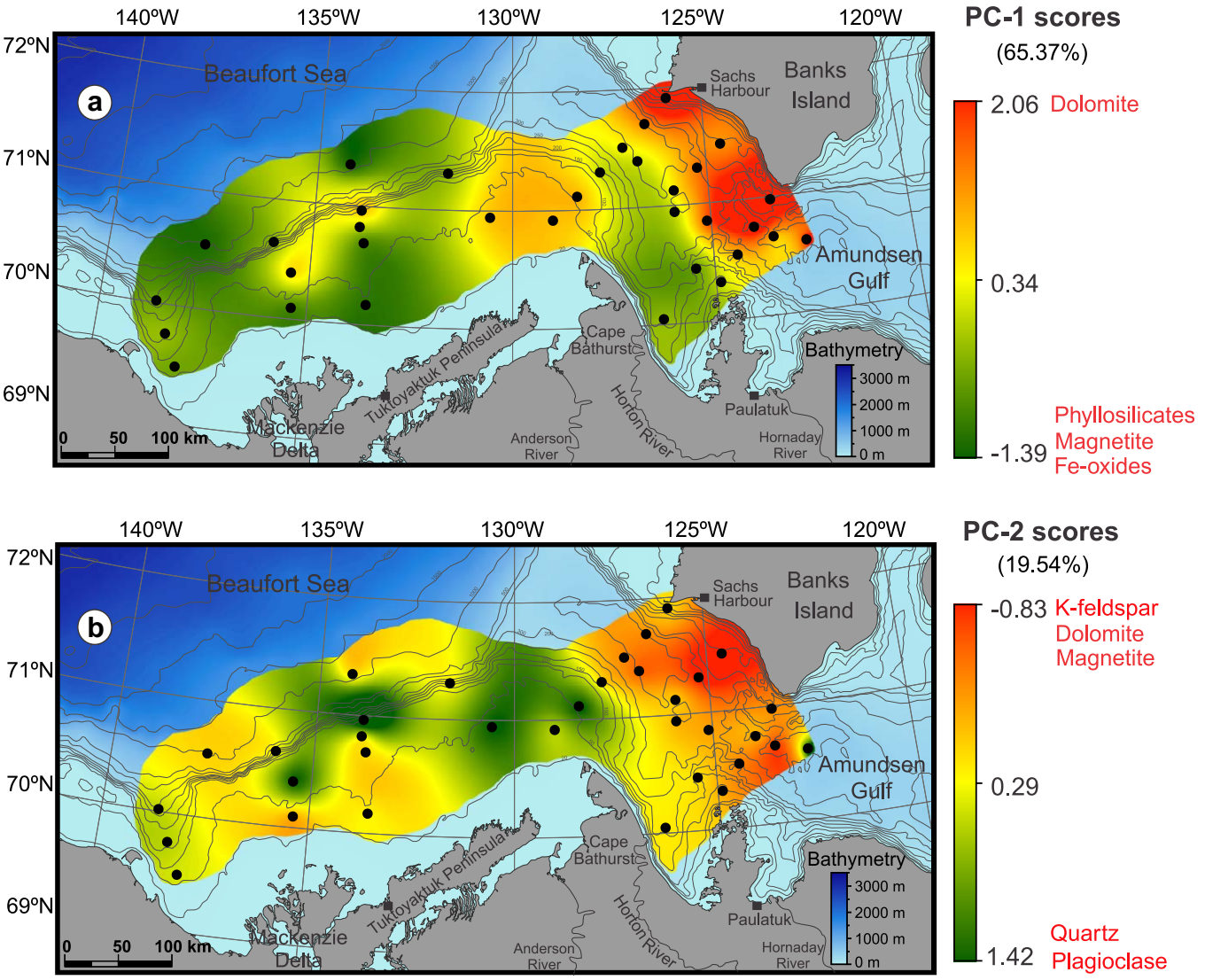

Figure 7. Map of PC-1 and PC-2 scores derived from the bulk mineralogical data from the Canadian Beaufort Shelf and Amundsen Gulf sediments.

4.4. Elemental Geochemistry

The major element composition (supporting information Figure S2) in the Mackenzie Trough-Canadian Beaufort Shelf and Amundsen Gulf sediments is dominated by Si (25–37 wt.%), Al (4–10 wt.%), Ti (0.2–0.5 wt.%), Ca (1–8 wt.%), Fe (2–6 wt.%), K (1–3 wt.%), Mg (0.6–5 wt.%), P (0.2–0.8 wt.%), and Mn (0.02–2.2 wt.%), while the minor and trace elements are dominated by V (120–325 μg/g), Zr (134–227 μg/g), Sr (107–209 μg/g), Zn (84–205 μg/g), and Cr (81–163 μg/g). LOI values range from 3 to 17.5 wt.%.

The ternary plot Al_2O_3-SiO_2-CaO (Figure 8a) illustrates that the sediments from the Mackenzie Trough-Canadian Beaufort Shelf are dominantly composed of detrital material similar to average shale, whereas the central Amundsen Gulf and southwestern Banks Island sediments show higher detrital carbonate contents (dolomite) and plot along the mixing line from average shale to the detrital carbonate end-member. Some sediment samples from the mud volcanoes (samples 403, 609, and 709) and central Amundsen Gulf (sample 106) are enriched in quartz (SiO_2 >45%; Figure 8a). Furthermore, Fe/Al and Mn/Al display a high positive linear correlation ($r = 0.75$; Figure 8b), indicating a geochemical relationship most likely similar to Fe–Mn oxyhydroxide phases. The enrichment factors of redox-sensitive elements (V, Cr, Zn) reveal modest authigenic enrichment (1–3) in all sedimentological provinces compared to average shale values (Figure 9). Fe shows no detectable authigenic enrichment in any sediment samples, whereas Mn has moderate-to-strong

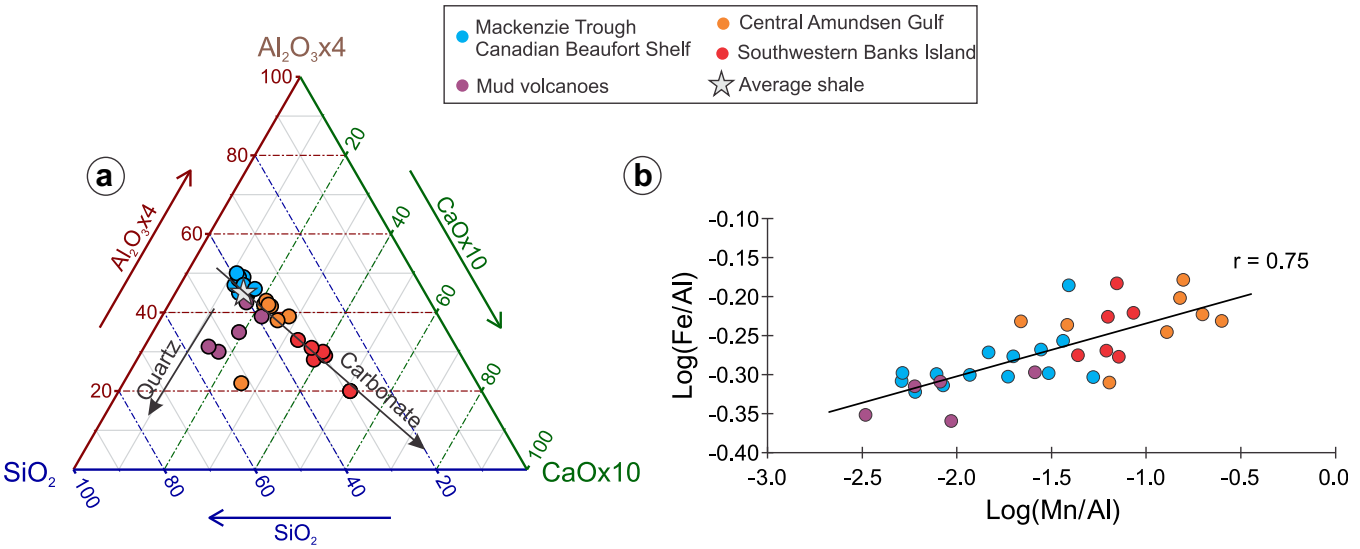

Figure 8. (a) Al_2O_3-SiO_2-CaO ternary plot shows the overall composition of surface sediments from the Canadian Beaufort Shelf and Amundsen Gulf in comparison with average shale (adapted from *Brumsack* [1989]). (b) Log(Fe/Al) versus Log(Mn/Al).

authigenic enrichment (EF > 5) in the central Amundsen Gulf and southwestern Banks Island and modest enrichment (EF < 3) in the Mackenzie Trough-Canadian Beaufort Shelf.

Principal component analyses based on these major, minor, and trace elements (Figure 10a) reveal that the PC-1 scores (71.05% of the total variance) are positively associated with Ca-Mg-LOI and negatively associated with Al-K-Ti-Fe-Cr-V-Zn-P, whereas the PC-2 scores (11.27% of the total variance) are positively associated with Si-Zr-Cr-Ca-P and negatively associated with K-Fe-V-Mg-LOI (Figure 10b). Importantly, Mn was not employed in the PCA because of the large influence on the geochemical variability. The Mn surface distribution show higher concentrations in central Amundsen Gulf and southwestern Banks Island sediments

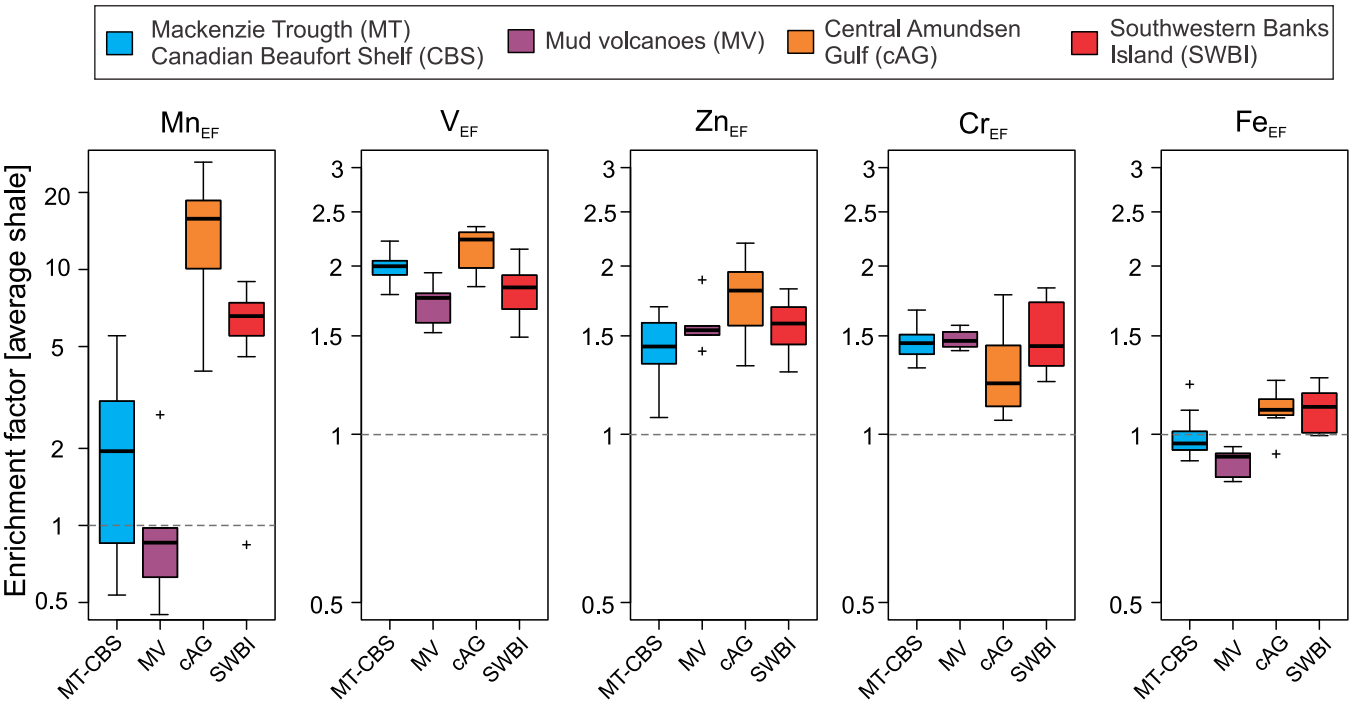

Figure 9. Box plots of the enrichment factors (EF) of redox-sensitive elements (Mn, Fe, V, Cr, Zn) from the Mackenzie Trough-Canadian Beaufort Shelf (MT-CBS), central Amundsen Gulf (cAG), and southwestern Banks Island (SWBI) sediments.

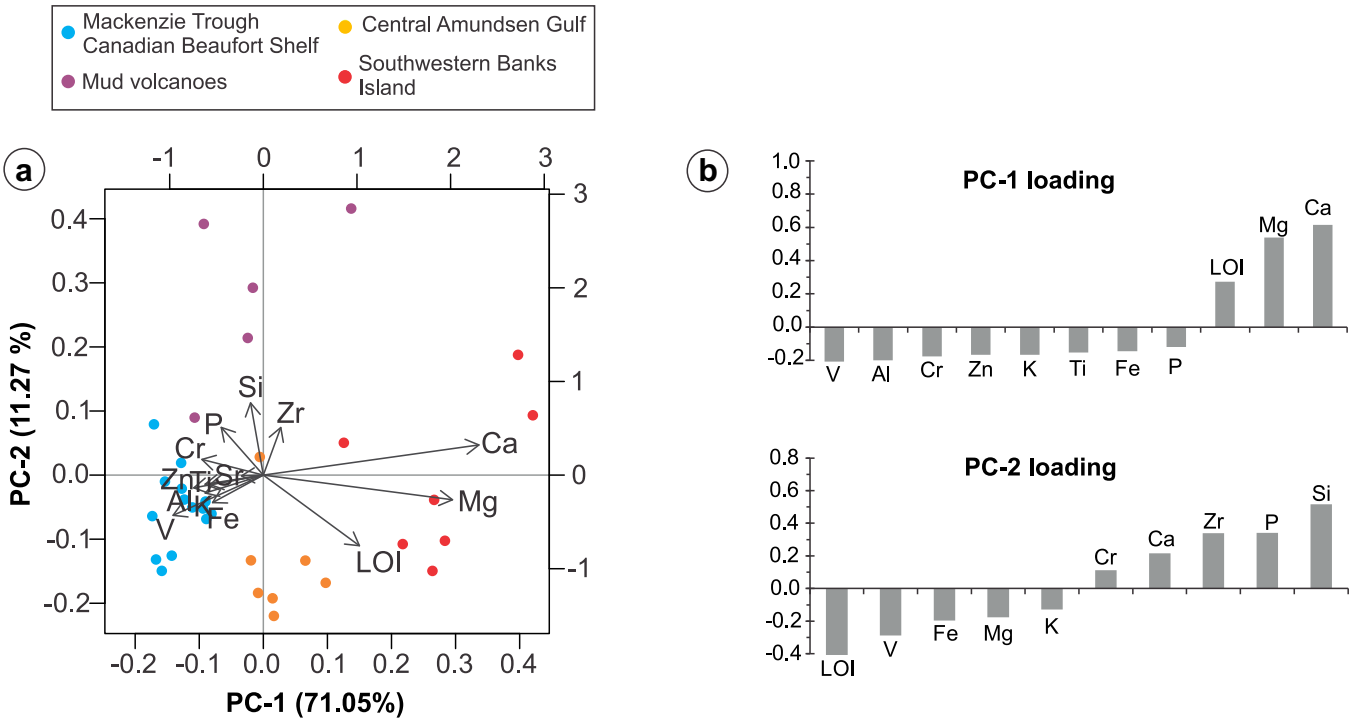

Figure 10. (a) Biplot of the PC-1 versus PC-2 obtained from the log-centered transformation of the major, minor, and trace-element data from the Canadian Beaufort Shelf and Amundsen Gulf sediments. (b) Loadings derived from the principal component analysis illustrating the weight (>0.1) of each element in the definition of each PC score.

compared to the Canadian Beaufort Shelf (Figure 11a). Moreover, the spatial distributions of the PC-1 and PC-2 elemental geochemical scores (Figures 11b and 11c) reveal similar trends as those observed in the bulk minerals (Figure 7), with large positive PC-1 scores (Ca-Mg-LOI) in the southwestern Banks Island and central Amundsen Gulf provinces and large negative PC-1 scores (Al-K-Ti-Fe-Cr-V-Zn-P) in the Mackenzie Trough-Canadian Beaufort Shelf province. Some coarse multimodal samples from the mud volcano province are characterized by positive PC-2 scores, which are associated with Si-Zr-Cr and Ca-P (Figure 11b).

SEM-EDS analysis performed on white crusts observed in mud volcano sediments (e.g., station 609; supporting information Figure S3) reveal Ca-Mg peaks, suggesting that these white crusts most probably represent authigenic carbonate minerals (notably, low Mg-calcite and/or dolomite). In addition, authigenic iron sulfides (such as pyrite and greigite) were not observed in the bulk sediment particles in the SEM-EDS analysis.

4.5. Relationship Between Grain Size, Bulk Mineralogy, Elemental Geochemistry, and Magnetic Properties

In order to explore the relationship among the grain size and PC scores from the bulk mineralogy and elemental geochemistry, a bivariate correlation was conducted (Figure 12). Note that sediment samples from the mud volcano province were not plotted because they are formed by different sedimentary processes. PC-1 scores derived from bulk mineralogy and elemental geochemistry exhibit a good to modest negative correlation with the mean grain size on the phi-scale, respectively (Figures 12a and 12b). This correlation suggests that variations in the mineralogical and geochemical signatures of surface sediments from the Mackenzie Trough-Canadian Beaufort Shelf and Amundsen Gulf are not only dominated by the relative contribution of the different sediment sources, but are also a function of grain-size sorting. In fact, a west-east trend in sediment composition and grain size may be observed in Figures 2a, 3a, 4c, 5c, and 12a–12c. In the Mackenzie Trough-Canadian Beaufort Shelf sediments, the phyllosilicate-Fe-oxide-magnetite (negative PC-1 scores from XRD) and Al-K-Ti-Fe-Cr-V-Zn-P (negative PC-1 from XRF) contents are highest in the clay to very fine silt fraction ($7.5<\phi<8.5$), whereas dolomite−K-feldspar (positive PC-1 scores from XRD) and Ca-Mg-LOI (positive PC-1 scores from XRF) contents are highest in the very fine to fine silt fraction ($6.5<\phi<7.5$) of the southwestern Banks Island sediments. Interestingly, there is a weak negative correlation with the mean grain size in phi units for the magnetic susceptibility (k_{LF}) (Figure 12c), suggesting that the k_{LF} variability can

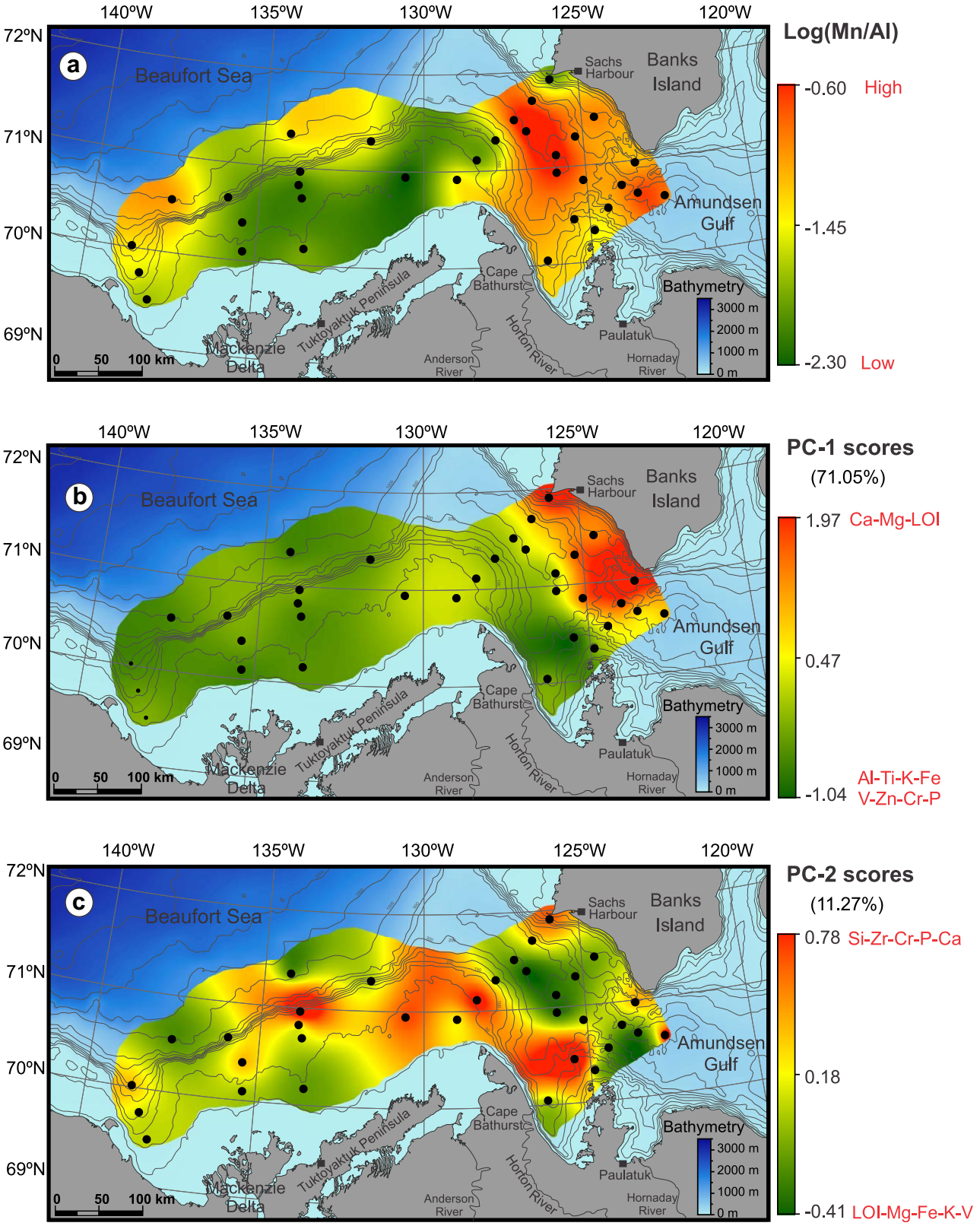

Figure 11. (a) Spatial distribution of Log(Mn/Al). (b and c) Map of PC-1 and PC-2 scores derived from the major, minor, and trace-element data from the Canadian Beaufort Shelf and Amundsen Gulf sediments.

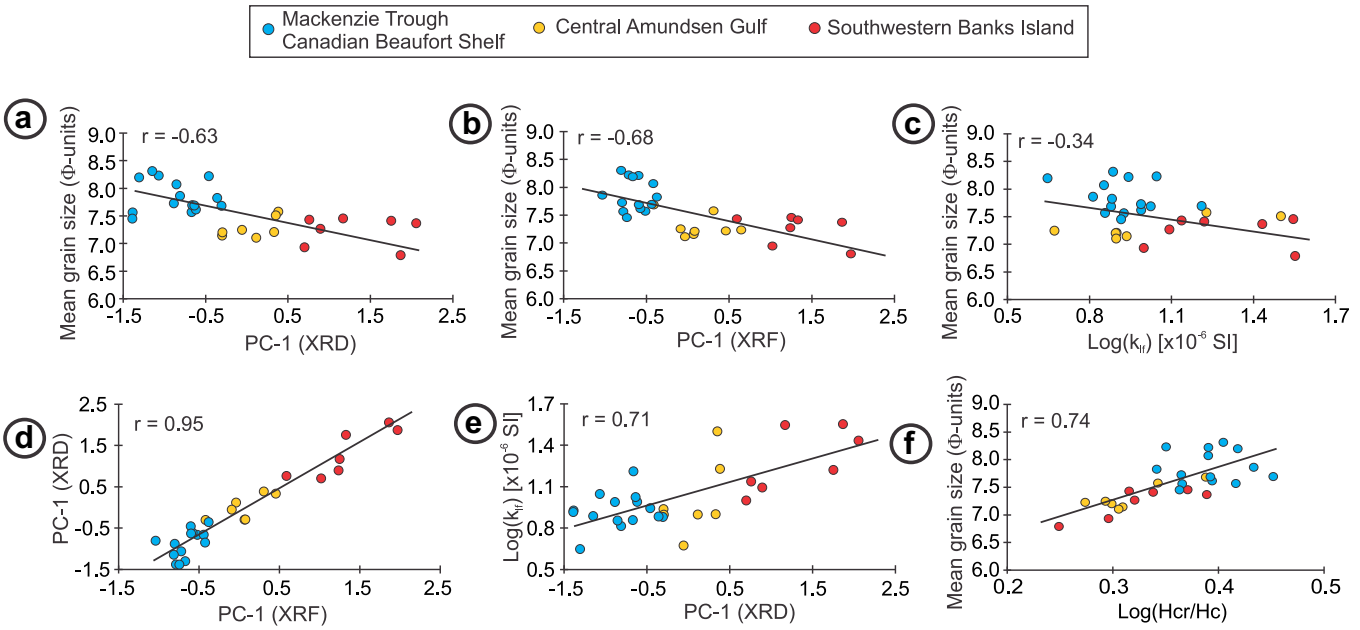

Figure 12. Relationship between siliciclastic mean grain size (phi units), bulk mineralogy (PC-1 score), elemental geochemistry (PC-1 score), magnetic susceptibility [Log(k_{lf})], and Log(Hcr/Hc).

only partly be explained by the grain-size sorting. In general, the lowest k_{LF} is recorded in the clay to very fine silt fraction, where the magnetite and Fe-oxide contents are highest (Figure 6a), with an inverse trend observed in the fine silt fraction.

To explore the relationship among the magnetic susceptibility (k_{LF}) and the mineralogical and geochemical signatures in the surface sediments, a bivariate correlation was also performed. A good positive correlation is observed between all detrital proxies used here (Figures 12d–12f), suggesting that: (1) the minerals and chemical composition of detrital particles are highly intercorrelated, and thus, phyllosilicates-Fe-oxides-magnetite are associated with Al-K-Ti-Fe-Cr-V-Zn-P contents, whereas dolomite-K-feldspar are associated with Ca-Mg-LOI contents; and (2) magnetic minerals (notably, magnetite) are derived mainly from detrital sources.

Since the distribution of geochemical elements in the Canadian Beaufort Sea-Amundsen Gulf region is closely linked to the mineralogical distribution (Figure 12e), either may be used to discriminate regional groups (or provinces) with a different sedimentary composition. Consequently, we performed a fuzzy c-means clustering analysis based on four unassociated key minerals (quartz−phyllosilicates-K-feldspar-dolomite; Figure 6a) to ascertain whether the differences between each predefined province are statistically valid. The ordination diagram and silhouette plots corroborates that sediment samples can be divided into four homogeneous clusters or sedimentary provinces (Figure 13), as indicated by their relatively high membership value (up to 0.60; Figure 13b): (1) Mackenzie Trough-Canadian Beaufort Shelf, (2) southwestern Banks Island, (3) central Amundsen Gulf, and (4) mud volcanoes.

5. Discussion

The spatial variations observed in the siliciclastic grain size, magnetic properties, mineralogical, and geochemical record from the Mackenzie Trough-Canadian Beaufort Shelf and Amundsen Gulf sediments are likely related to changes in redox conditions, surface detrital provenance, and sediment dispersal of the land-derived particles delivered by the Mackenzie River to the shelf and coastal erosion.

5.1. Sedimentary Redox Conditions

Given that Mn forms a highly insoluble oxyhydroxide where oxic conditions prevail [*Burdige*, 1993; *Calvert and Pedersen*, 2007], the moderate to strong degree of Mn enrichment (EF > 5) in the central Amundsen Gulf and southwestern Banks Island sediments compared to the Canadian Beaufort Shelf suggests that

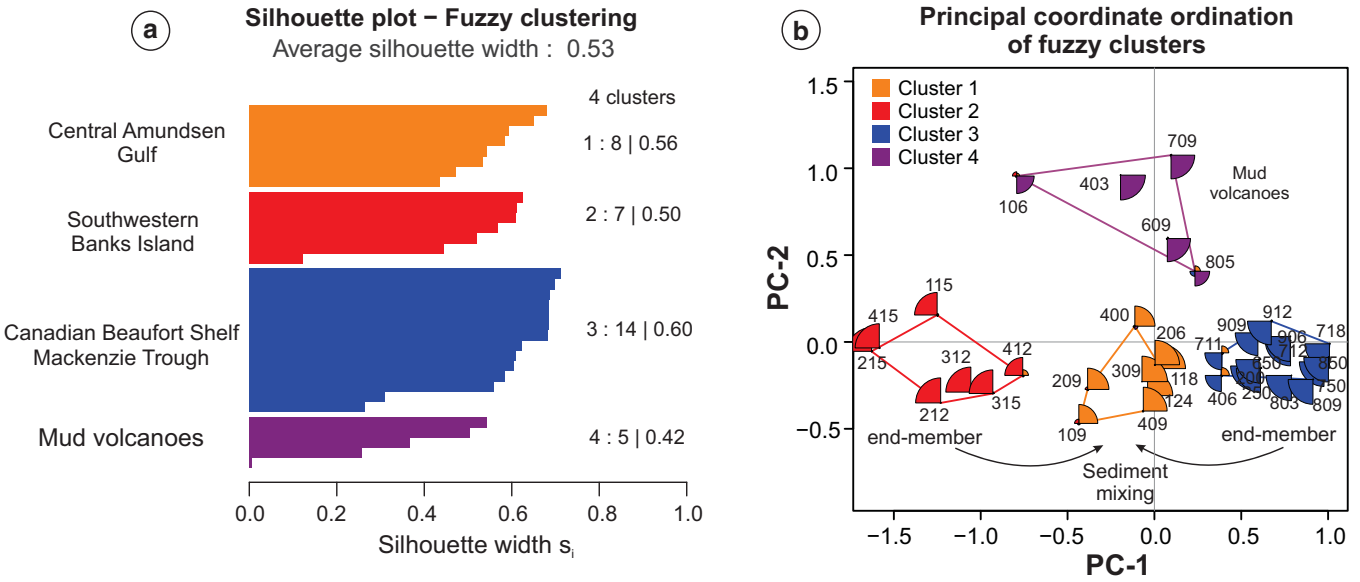

Figure 13. (a) Silhouette and (b) principal coordinate ordination plots resulting from the fuzzy c-means clustering analysis based on the bulk mineralogical data from the Canadian Beaufort Shelf and Amundsen Gulf sediments. The parameters listed on the right-hand side in Figure 13a represent of number of sample in each cluster and their membership's values. 100% of the cluster memberships are correctly classified. In Figure 13b each cluster is associated with a small "star" whose segment radiuses are proportional to its membership coefficient.

more oxic conditions prevail at the sediment-water interface in this area (Figures 9 and 11a). In agreement with previous geochemical studies [e.g., *O'Brien et al.*, 2006; *Mucci et al.*, 2010; *Tremblay et al.*, 2014], we hypothesize that these differences in oxic conditions are likely related with more turbulent mixing of the water column. Indeed, despite the pronounced stratification [*Tremblay et al.*, 2014], strong winds in conjunction with recurrent ice-free conditions for much of the year likely led to strong vertical mixing within Amundsen Gulf. These conditions produce a well-oxygenated water column, but also promote the settling of Fe-Mn oxyhydroxide particles onto the seafloor [e.g., *Macdonald and Gobeil*, 2012]. Conversely, on the Canadian Beaufort Shelf, the large supply of terrigenous organic matter from the Mackenzie River keeps the oxic-anoxic boundary close to the sediment-water interface and allows the reductive remobilization and release of Fe and Mn from oxyhydroxide coatings into the uppermost sediments and overlying water column [*Magen*, 2007; *Magen et al.*, 2011]. Alternatively, the high Mn-enrichment factors found in the central Amundsen Gulf and southwestern Banks Island (Figure 9) may also be related to the lower detrital Al-rich minerals (Figure 8b) received in these zones as no large rivers discharge into Amundsen Gulf and only a small amount of the Mackenzie River sediment plume reaches the Gulf [e.g., *Hill et al.*, 1991; *Macdonald et al.*, 1998]. However, as shown in Figure 9, redox-sensitive elements (Fe, V, Cr, Zn) are not authigenically enriched (EF <3), supporting the idea that predominantly oxic conditions prevail at the sediment-water interface [e.g., *Magen*, 2007]. Accordingly, these redox-sensitive elements reveal a good association with Al, advocating a mostly detrital origin (Figure 10a).

5.2. Sedimentary Provinces and Sediment Provenance

The spatial distribution of principal component scores, together with fuzzy c-means clustering analysis, indicates that there are four provinces with distinct sedimentary compositions within the Mackenzie Trough-Canadian Beaufort Shelf and Amundsen Gulf, as described below.

5.2.1. Mackenzie Trough-Canadian Beaufort Shelf

This sedimentary region is the most widespread and is characterized by mineral (phyllosilicates, Fe-oxides, magnetite) and element (Al-K-Ti-Fe-Cr-V-Zn-P) associations mainly found in the fine-grained aluminosilicate and Fe-Mn oxide fractions. The variability in detrital input delivered to the Canadian Beaufort Shelf via the Mackenzie River discharge and the subsequent hydraulic sorting most probably controls the distribution and accumulation of these minerals and elements. Note that sediment contribution to the Canadian Beaufort Sea by the Arctic Alaskan rivers and coastal erosion is relatively small compared to the Mackenzie River discharge [*Hill et al.*, 1991]. Likewise, with the exception of the mud volcano areas, the PC scores from both bulk mineralogy and elemental geochemistry (Figures 7 and 11b, c), as well as the Al-Si-Ca relationship

(Figure 8a), exhibit a homogeneous sedimentary composition within this province. This homogeneity suggests a common detrital particle provenance and supports the notion that the Mackenzie River sediment plume has a wide easterly propagation, thus influencing modern sedimentation in the entire Canadian Beaufort Shelf area [e.g., *Hill et al*., 1991; *Carmack and Macdonald*, 2002; *Richerol et al*., 2008b].

The overall mineralogical and geochemical signatures characterizing this province, point to a detrital input from a more aluminosiliciclastic-carbonate sedimentary source such as the Cambrian to Cretaceous shales, sandstones, and limestone cropping out in the Interior Platform. This assumption is in agreement with the Sr isotope composition of suspended sediments from the Mackenzie basin [*Millot et al*., 2003], suggesting that the Mackenzie River system is mostly dominated by the tributaries of the Interior Plain, with the northern Rockies and Mackenzie Mountains as secondary sources. In addition, compared to the rivers of the Mackenzie and Rocky Mountains, those of the interior plains also supply large amounts of terrestrial organic matter to the Canadian Beaufort Shelf [*Millot et al*., 2003], almost all of which (~97%) is deposited on the inner to middle shelf [*Macdonald et al*., 1998; *O'Brien et al*., 2006]. Accordingly, the slightly lower magnetic susceptibility (k_{lf}) values in this province, where the iron-bearing mineral (magnetite and Fe-oxides) contents are highest, may be accounted for by a dilution effect from a high organic-matter supply [e.g., *Bloemendal et al*., 1992]. The large amounts of terrigenous organic material deposited on the Canadian Beaufort Shelf compared to Amundsen Gulf [e.g., *Macdonald et al*., 1998; *Magen et al*., 2010], lead to organic matter diluting the magnetic fine-grained material and, therefore, producing low magnetic susceptibility (k_{lf}) values.

5.2.2. Southwestern Banks Island

This province is characterized mainly by the association of dolomite-K-feldspar and Ca-Mg-LOI and, to a lesser extent, by phyllosilicates, Fe-oxides and Mn (Figures 7 and 11a–11c). Likewise, fine silt contents are higher in this province compared to the Mackenzie Trough-Canadian Beaufort Shelf area (Figures 2a and 3c). Since biogenic carbonates are only of subordinate importance (calcite <1%), detrital carbonate (dolomite) is the main host mineral for Ca-Mg-LOI (Figures 7 and 11). In agreement with petrographic and bulk mineralogy studies performed around Banks Island [e.g., *Bader and Henry*, 1961; *Bischof et al*., 1996; *Vogt*, 1997], we hypothesize that most of the fine silt detrital sediments in this province are mainly supplied from coastal cliff erosion of fine-grained Pleistocene carbonate-rich glacial tills and clastic sedimentary rocks cropping out on southwestern Banks Island. In fact, much of the coastline along southwestern Banks Island and Amundsen Gulf is vulnerable to coastal erosion [*O'Brien et al*., 2006]. According to *Belliveau* [2007], the summer melting of ground ice on the southwestern coast of Banks Island generally leads to slumping along coastal cliffs, which not only creates large erosional areas, but also increases the amount of fine-grained sediments available that can reach the coastline, especially during the open-water season (June–September) when southeast winds and onshore storm winds predominate.

Compared to the Mackenzie Trough-Canadian Beaufort Shelf province, this zone has a less-extended modern detrital contribution to the eastern part of Amundsen Gulf (Figures 7a and 11b). Note, however, that from a more regional perspective and based on the geochemical fingerprint of entrained Fe-oxide mineral grains in Arctic Ocean sea ice, *Darby* [2003] suggests that the Banks Island shelf is the most important source of sediment accumulated from ice floes in the Beaufort Sea, northern Chukchi Sea, and the Chukchi Borderland area. Indeed, easterly winds dominate the ice-cover dynamics in the Canadian Beaufort Sea region [*Hill et al*., 1991] and promotes a recurrent polynya (known as the Cape Bathurst Polynya) [*Arrigo and van Dijken*, 2004] on the southwestern coast of Banks Island (Figure 1). In this shallow, ice-free area, stronger winds in fall and winter induce turbulent mixing of the water column, leading to both a more oxygenated water column and the recurrent incorporation of shelf sediments into the sea ice (a process known as suspension freezing) [*Reimnitz et al*., 1993]. These sea ice and ice floes are subsequently transported westward of the area via surface currents and the clockwise BG current system [*Darby*, 2003].

5.2.3. Central Amundsen Gulf

This province represents a transitional zone between the Mackenzie Trough-Canadian Beaufort Shelf and southwestern Banks Island sedimentary provinces and is characterized by intermediate phyllosilicate-magnetite-dolomite-K-feldspar and Al-K-Ti-Fe-Mn-V-Zn-Sr-Ca-Mg-LOI contents (Figures 7 and 11). Similarly to southwestern Banks Island sediments, fine silt contents are also higher in this province compared to the Mackenzie Trough-Canadian Beaufort Shelf area (Figures 2a and 3a). Thus, this zone consists mainly of minerals and elements resulting from a mixture of (1) the aluminosiliciclastic and iron-bearing material likely derived from the Mackenzie River discharge and (2) detrital carbonate and K-feldspar derived from coastal

erosion of southwestern Banks Island. Indeed, resuspended shelf sediment and sediment from the Mackenzie River discharge may reach Amundsen Gulf in the summer when northwesterlies dominate [*O'Brien et al*., 2006]. In contrast, because southwestern Banks Island is not influenced by significant river discharges, coastal cliff erosion plays a more important role in sediment supply and transport to the central Amundsen Gulf [*Belliveau*, 2007]. Alternatively, we cannot rule out that other secondary source rivers, such as the Horton and Hornaday rivers (Figure 1), might also reach the Amundsen Gulf during break-up in the spring. Furthermore, because the drainage basin of these rivers is covered by Palaeozoic sedimentary rocks as well as fine-grained Pleistocene potassium-rich glacial till resulting from the glacial erosion of Precambrian Canadian Shield rocks [e.g., *Padgham and Fyson*, 1992], they may also supply quartz and K-feldspar minerals to the Gulf.

5.2.4. Mud Volcanoes

This province is characterized by poorly sorted medium to fine silt sediments (Figures 2b and 3c) with high quartz-plagioclase, authigenic carbonate (low Mg-calcite and/or dolomite; Figure 7 and supporting information Figure S3), and Si-Zr (Figure 11) contents, as well as high magnetic susceptibility values (Figure 5a). As no large rivers discharge to the east Mackenzie River (R-ArcticNet database) and coastal erosion is only an important local sediment supply near the shoreline in the Canadian Beaufort Shelf [*Carmack and Macdonald*, 2002], we hypothesize that detrital sediments supply within these specific areas are driven by the mud volcanoes activity. Based on seismic stratigraphy studies performed along the eastern Canadian Beaufort Shelf [*Blasco et al*., 1990; *Hill et al*., 1991; *Batchelor et al*., 2013] and submarine mud volcano distribution [*Blasco et al*., 2013], we presume that the detrital sediment in these areas derived from the subsurface sediment remobilization of the fine-grained Pleistocene quartz-rich glacial tills deposited in the Shelf following mud migration toward the surface. Indeed, fluidized/gasified sediment eruptions associated with the mud volcanoes activity promote the remobilization and transport to the seafloor of the sediments accumulated in the subsurface [*Paull et al*., 2007, 2015]. This interpretation is in agreement with previous studies on the mud volcanoes from the Canadian Beaufort Shelf [e.g., *Paull et al*., 2007; *Blasco et al*., 2013; *Paull et al*., 2015] that suggest that the crest sediments are significantly older than the moat sediments and they almost certainly predate the marine transgression [*Hill et al*., 1993]. In addition, the mud volcanoes are also most likely responsible for the higher magnetic susceptibility values in these areas. Lower ratios of Mrs/Ms and higher ratios of Hcr/Hc suggest that mud volcanoes sediments are dominated by coarser magnetite grains (Figure 4), which are responsible for the increase in magnetic susceptibility recorded within this province. This is consistent with the remobilization of fine till material toward the surface by the mud volcanos activity.

On the other hand, the high authigenic carbonate contents observed in this province may be related with the gas hydrate decomposition [*Moore et al*., 2004; *Lu et al*., 2014]. In fact, ascending venting methane derived from the gas hydrate decomposition come in contact with seawater sulfate near the seafloor, where an anaerobic oxidation of methane takes place, favoring the authigenic carbonate precipitation (which may include calcite, dolomite, and/or aragonite). This environmental process has been proposed to operate in different mud volcanoes settings from Fram Strait [*Ambrose et al*., 2015], South China Sea [*Lu et al*., 2014], Niger deep-sea fan [*Bayon et al*., 2007], and Mediterranean [*Pancost et al*., 2001], among others.

To summarize, the spatial trends of our mineralogical, geochemical, and magnetic data, together with the fuzzy c-means clustering analysis, suggest that: (1) the Mackenzie River discharge is the main contributor of terrigenous sediments in the entire Canadian Beaufort Shelf, (2) southwestern Banks Island represents a secondary source of sediments in the central Amundsen Gulf, (3) sediments from the central Amundsen Gulf represent a mix of sediments derived from both the Mackenzie River discharge and coastal erosion of southwestern Banks Island, and (4) the Canadian Beaufort Shelf area is preferentially influenced by mud volcano activity (see summary in Figure 14).

5.3. Comparison to Other Circum-Arctic Regions: Mineralogical Clues

Continents surrounding the Arctic Ocean comprise bedrock/soils characterized by different petrographic signatures [e.g., *Vogt*, 1997; *Stein*, 2008; *Harrison et al*., 2008; *Bazhenova*, 2012; *Fagel et al*., 2014; *Linsen et al*., 2014]. Consequently, as suggested by *Vogt* [1997], surface sediments from circum-Arctic source areas may be characterized by very specific K-feldspar/plagioclase (Kfs/Plg) and quartz/(K-feldspar + plagioclase) (Qz/Fsp) ratios. To verify this notion, we compared our bulk mineralogical data with other circum-Arctic regions (Figure 15), notably with surface marine sediments from the Eurasian shelf [*Stein*, 2008; *Bazhenova*, 2012], Bering Strait [*Linsen et al*., 2014], as well as with continental sediments from the northern Yukon Territory,

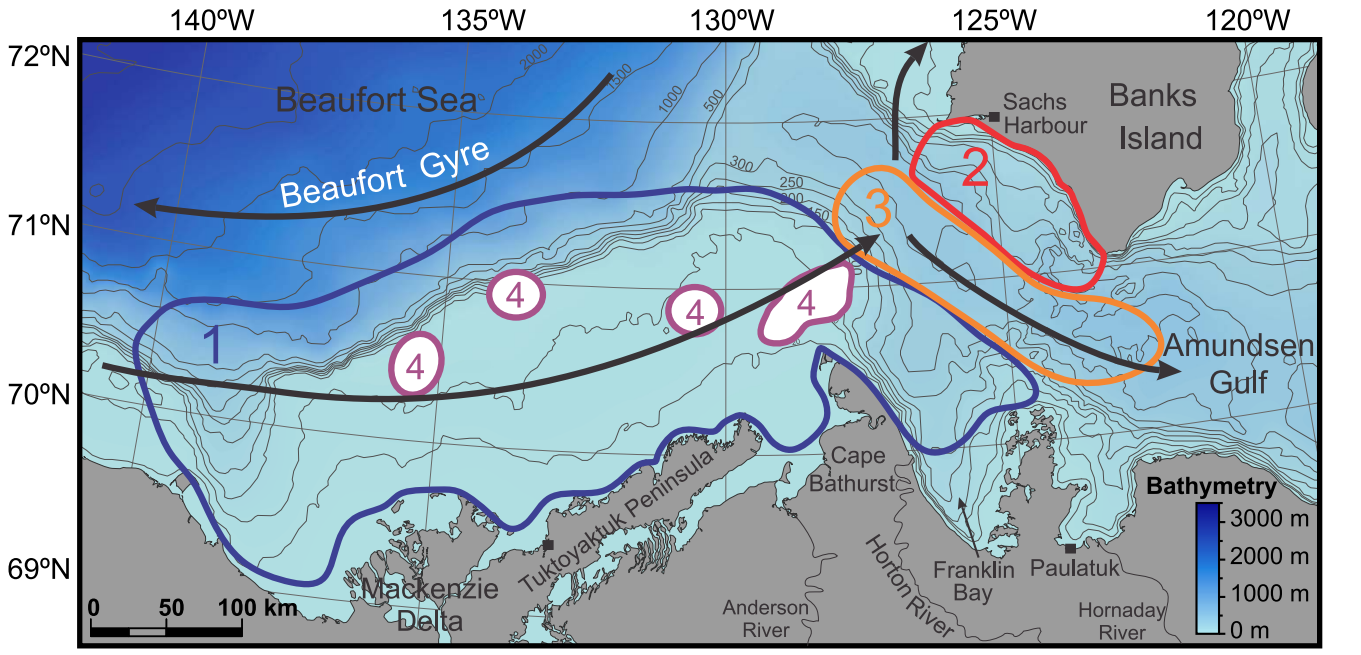

Sedimentary provinces:

1. Preferential influence of discharge of the Mackenzie River
   high phyllosilicates, Fe oxides, magnetite and Al-K-Ti-Fe-Cr-V-Zn-P contents
2. Preferential influence of coastal erosion
   high dolomite, K-feldspar and Ca-Mg-LOI contents
3. Transition zone (mixture characteristics from zones 1 and 2)
   intermediate phyllosilicates, magnetite, K-feldspar, dolomite, and Al-K-Ti-Fe-Mn-V-Zn-Sr-Ca-Mg-LOI contents
4. Zone influenced by mud volcanoes
   high quartz-plagioclase-authigenic carbonates and Si-Zr contents, high magnetic susceptibility

Figure 14. Generalized map summarizing the main sedimentary provinces defined in this study. The thick white arrows represent surface currents.

Tuktoyaktuk Peninsula, Cape Bathurst, and Banks Island [*Vogt*, 1997]. Our findings indicate that sediments from the Mackenzie Trough-Canadian Beaufort Shelf, Amundsen Gulf, and Banks Island have higher Qz/Fsp (2–4) and Kfs/Plg (>0.7) ratios compared to Eurasian sediments (Figure 15). In the study area, quartz and K-feldspar are mainly supplied by the Mackenzie River discharge (which drain large sedimentary platforms) and by coastal erosion of the Pleistocene potassium and carbonate-rich glacial till cropping out on south-western Banks Island. In contrast, rivers from the Eurasian margin drain large basaltic provinces that can supply high amounts of plagioclase [*Stein*, 2008]. Plagioclase weathers much faster than K-feldspar as silicate weathering preferentially attacks Na and Ca-rich minerals [*White et al.*, 2001]. In glacial environments, this implies that mechanical comminution of plagioclase is more effective than K-feldspar during the initial stages of feldspar weathering [e.g., *von Eynatten et al.*, 2016]. As a result, plagioclase is enriched over K-feldspar in the Eurasian shelf sediments compared to the Canadian Beaufort Shelf and Amundsen Gulf, and thus yields sediments with lower Qz/Fsp (0.2–1) and Kfs/Plg (0.2–0.7) ratios (Figure 15). On the other hand, sediment samples from the mud volcano province display higher Qz/Fsp (>3) ratios similar to the glacial tills cropping out along the northern Yukon Territory (VH83-014), Tuktoyaktuk Peninsula (VH85-045), and Cape Bathurst (VH85-006), suggesting a common detrital origin for these sediments, which likely originate from the glacial activity of the Laurentide Ice Sheet. These also support our interpretation that the mud volcano province are composed of glacial tills that have been remobilized from the subsurface of the Canadian

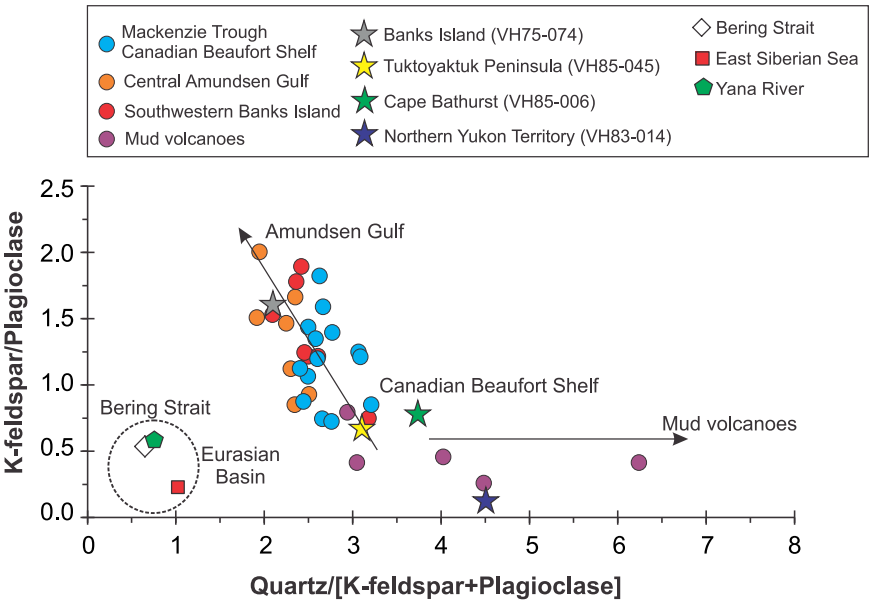

Figure 15. K-feldspar/plagioclase versus quartz/(K-feldspar + plagioclase) diagram illustrating the mineralogical difference between some circum-Arctic regions. Surface marine sediments from the Canadian Beaufort Sea (this study), Amundsen Gulf (this study), Eurasian shelf [*Stein*, 2008; *Bazhenova*, 2012], Bering Strait [*Linsen et al*., 2014], as well as continental sediments from the northern Yukon Territory, Tuktoyaktuk Peninsula, Cape Bathurst, and Banks Island [*Vogt*, 1997] are plotted.

Beaufort Shelf (see section 5.2.4.). Finally, little difference is observed between surface sediments from the Bering Strait and Eurasian sediments (Figure 15) because Bering Strait sediments also contain significant amounts of plagioclase that mainly originated from the Anadyr River drainage basin, where volcanic, granitic, and granodiorite rocks crop out [e.g., *Linsen et al*., 2014].

6. Conclusions

The spatial variability of continental input, surface currents, and redox conditions within the Mackenzie-Beaufort Sea Slope and Amundsen Gulf was investigated through analyses of the grain size, magnetic properties, and the mineralogical and geochemical composition of 34 surface sediment samples. The results of this research yield the following generalizations and conclusions:

1. The relative enrichment in redox-sensitive elements (Mn, Fe, V, Cr, Zn) suggests that modern sedimentary deposition within the Mackenzie-Beaufort Sea Slope and Amundsen Gulf took place under oxic bottom-water conditions;
2. Strong winds together with recurrent ice-free conditions for much of the year appear to be a plausible scenario for explaining the well-oxygenated water column and, therefore, the high Mn-enrichment factors observed in the Amundsen Gulf compared to the Canadian Beaufort Shelf;
3. The mineralogical, geochemical, and magnetic signatures of surface sediments allowed the identification of four provinces with distinct sedimentary compositions: (1) the Mackenzie Trough-Canadian Beaufort Shelf, characterized by minerals (phyllosilicates, Fe-oxides, magnetite) and elements (Al-K-Ti-Fe-Cr-V-Zn-P) derived mainly from the Mackenzie River discharges; (2) southwestern Banks Island, characterized by the association of dolomite-K-feldspar and Ca-Mg-LOI mainly supplied from coastal cliff erosion of Pleistocene potassium- and carbonate-rich glacial tills as well as clastic sedimentary rocks cropping out on the island; (3) the central Amundsen Gulf, which represents a transitional zone typified by intermediate phyllosilicates-magnetite-K-feldspar-dolomite and Al-K-Ti-Fe-Mn-V-Zn-Sr-Ca-Mg-LOI contents resulting from a detrital mix between the Mackenzie River discharges and coastal erosion of southwestern Banks Island; and (4) the mud volcanoes distinguished by the association quartz-plagioclase-authigenic carbonate and Si-Zr contents, as well as high magnetic susceptibility values resulting from the remobilization of glacial tills deposited in the subsurface of the Canadian Beaufort Shelf; and

4. Our mineralogical data corroborate that K-feldspar/plagioclase and quartz/(K-feldspar+plagioclase) ratios [*Vogt*, 1997], together with detrital carbonate (dolomite), can be successfully used to track changes in terrigenous sediment input from the Canadian Beaufort Sea, Eurasian shelf, and Bering Strait.

Taken as a whole, our data provide a baseline for future studies using the mineralogical, geochemical, and magnetic signatures of sediment cores from the Mackenzie-Beaufort Sea Slope and Amundsen Gulf in order to reconstruct and document past variations in continental inputs and sediment dispersal related to climate changes.

Acknowledgments
This research is a contribution to the Canadian Arctic Shelf Exchange Study (CASES) program and was funded by the Natural Sciences and Engineering Research Council of Canada (NSERC) through Discovery Grants and FQRNT "*Nouveau chercheur*" grants to J-C Montero-Serrano, G. St-Onge, and A. Rochon, as well as through Ship Time support for several expeditions (J-C Montero-Serrano, G. St-Onge, and A. Rochon). We also acknowledge the financial support of the Canadian Foundation for Innovation (CFI) and Canada Economic Development for Quebec Regions (CED) for the acquisitions of the PANalytical X-ray diffractometer (X'Pert Powder) and X-ray fluorescence (Epsilon 3-XL), respectively. We also thank Quentin Beauvais, Marie-Pier St-Onge, Elissa Barris, Julie Velle, and Claude Belzile from UQAR-ISMER for their technical support and advice. Finally, we thank Christine Laurin for reviewing the grammar and Stefanie Brachfeld and an anonymous reviewer for their constructive comments that helped improve the manuscript. All analytical data presented are available electronically in the PANGAEA database (https://doi.pangaea.de/10.1594/PANGAEA.866871).

References

Aagaard, K. (1984), The Beaufort undercurrent. In The Alaskan Beaufort Sea: Ecosystems and Environments, edited by Peter W. Barnes, Donald M. Schell and Erk Reimnitz, Academic Press, San Diego, California, pp. 47–71. http://dx.doi.org/10.1016/B978-0-12-079030-2.50009-5

Aitchison, J. (1986), *The Statistical Analysis of Compositional Data. Monographs on Statistics and Applied Probability*, Chapman and Hall, London, U. K. (Reprinted in 2003 with additional material by The Blackburn Press).

Aitchison, J. (1990), Relative variation diagrams for describing patterns of compositional variability, *Math. Geol.*, *22*, 487–511, doi:10.1007/BF00890330.

Ambrose, W. G., G. Panieri, A. Schneider, A. Plaza-Faverola, M. L. Carroll, E. K. L. Åström, WL. Locke, and J. Carroll (2015), Bivalve shell horizons in seafloor pockmarks of the last glacial-interglacial transition: A thousand years of methane emissions in the Arctic Ocean, *Geochem. Geophys. Geosyst.*, *16*, 4108–4129, doi:10.1002/2015GC005980.

Arrigo, K. R., and G. L. van Dijken (2004), Annual cycles of sea ice and phytoplankton in Cape Bathurst polynya, southeastern Beaufort Sea, Canadian Arctic, *Geophys. Res. Lett.*, *31*, L08304, doi:10.1029/2003GL018978.

Asahara, Y., F. Takeuchi, K. Nagashima, N. Harada, K. Yamamoto, and K. Oguri, and O. Tadai (2012), Provenance of terrigenous detritus of the surface sediments in the Bering and Chukchi Seas as derived from Sr and Nd isotopes: Implications for recent climate change in the Arctic regions, *Deep Sea Res., Part II*, *61–64*, 155–171, doi:10.1016/j.dsr2.2011.12.004.

Bader, R. G., and V. J. Henry (1961), Marine sediments of Prince of Wales Strait and Amundsen Gulf, West Canadian Arctic, *J. Mar. Res.*, *17*, 35–52.

Barber, D. G., and J. M. Hanesiak (2004), Meteorological forcing of sea ice concentrations in the southern Beaufort Sea over the period 1979 to 2000, *J. Geophys. Res.*, *109*, C06014, doi:10.1029/2003JC002027.

Barletta, F., G. St-Onge, J. E. T. Channell, A. Rochon, L. Polyak, and D. Darby (2008), High-resolution paleomagnetic secular variation and relative paleointensity records from the western Canadian Arctic: Implication for Holocene stratigraphy and geomagnetic field behaviour, *Can. J. Earth Sci.*, *45*, 1265–1281, doi:10.1139/E08-039.

Barletta, F., G. St-Onge, J. E. T. Channell, and A. Rochon (2010), Dating of Holocene western Canadian Arctic sediments by matching paleomagnetic secular variation to a geomagnetic field model, *Quat. Sci. Rev.*, *29*, 2315–2324, doi:10.1016/j.quascirev.2010.05.035.

Barris, E. (2012), Étude paléomagnétique des sédiments holocénes de la Fosse du Mackenzie, mer de Beaufort, MSc thesis, 97 pp., Inst. des sciences de la mer de Rimouski, Univ. du Québec à Rimouski, Rimouski, Que., Canada.

Batchelor, C. L., J. A. Dowdeswell, and J. T. Pietras (2013), Seismic stratigraphy, sedimentary architecture and palaeo-glaciology of the Mackenzie Trough: Evidence for two Quaternary ice advances and limited fan development on the western Canadian Beaufort Sea margin, *Quat. Sci. Rev.*, *65*, 73–87, doi:10.1016/j.quascirev.2013.01.021.

Bayon, G., C. Pierre, J. Etoubleau, M. Voisset, E. Cauquil, T. Marsset, N. Sultan, E. Le Drezen, and Y. Fouquet (2007), Sr/Ca and Mg/Ca ratios in Niger Delta sediments: Implications for authigenic carbonate genesis in cold seep environments, *Mar. Geol.*, *241*, 93–109, doi:10.1016/j.margeo.2007.03.007.

Bazhenova, E. (2012), Reconstruction of late Quaternary sedimentary environments at the southern Mendeleev Ridge (Arctic Ocean), PhD thesis, 83 pp., Univ. of Bremen, Bremen. [Available at urn:nbn:de:gbv:46-00102884-17.]

Belliveau, K. D. (2007), *Coastal Geomorphology of Southwest Banks Island, Northwest Territories: Historical and Recent Shoreline Changes and Implications for the Future*. MSc thesis, Department of Geography, Memorial University of Newfoundland, St. John's, Newfoundland, 247 pp. [Available at http://research.library.mun.ca/id/eprint/10153.]

Bennett, R., A. Rochon, T. Schell, J. Bartlett, S. Blasco, J. Hughes-Clarke, D. Scott, A. Macdonald, and W. Rainey (2008), Cruise Report Amundsen 2004-804: Beaufort Sea/Amundsen, *Geol. Surv. of Can. Open File, 5798*, 111 pp.

Bischof, J., D. L. Clark, and J.-S. Vincent (1996), Origin of ice-rafted debris: Pleistocene paleoceanography in the western Arctic Ocean, *Paleoceanography*, *11*, 743–756, doi:10.1029/96PA02557.

Bischof, J. F., and D. A. Darby (1999), Quaternary ice transport in the Canadian Arctic and extent of Late Wisconsinan Glaciation in the Queen Elizabeth Islands, *Can. J. Earth Sci.*, *36*, 2007–2022, doi:10.1139/e99-096.

Blasco, S., et al. (2013), 2010 State of knowledge: Beaufort Sea seabed geohazards associated with offshore hydrocarbon development, *Geol. Surv. Canada, Open File 6989*, 340 p., doi:10.4095/292616.

Blasco, S. M., G. Fortin, P. R. Hill, M. J. O'Connor, and J. Brigham-Grette (1990), The late Neogene and Quaternary stratigraphy of the Canadian Beaufort continental shelf, *in The Geology of North America*, vol. L, the Arctic Ocean Region, edited by A. Grantz, L. Johnson, and J. F. Sweeney, pp. 491–501, Geol. Soc. of Am., Boulder, Colo.

Bloemendal, J., J. W. King, F. R. Hall, and S.-J. Doh (1992), Rock magnetism of Late Neogene and Pleistocene deep-sea sediments: Relationship to sediment source, diagenetic processes, and sediment lithology, *J. Geophys. Res.*, *97*, 4361–4375.

Blott, S. J., and K. Pye (2001), Gradistat: A grain size distribution and statistics package for the analysis of unconsolidated sediments, *Earth Surf. Processes Landforms 26*, 1237–1248, doi:10.1002/esp.261.

Borcard, D., F. Gillet, and P. Legendre (2011), *Numerical Ecology with R*, 306 pp., Springer, New York.

Bornhold, B. D. (1975), Suspended matter in the southern Beaufort Sea. Beaufort Sea Project, *Tech. Rep. 25b*, 34 pp., Dep. of the Environ., Victoria, B. C.

Brachfeld, S., F. Barletta, G. St-Onge, L. Polyak, and D. Darby (2009), Environmental magnetic record of Holocene climate along the Alaska Chukchi Margin, *Global Planet. Change*, *68*, 100–114.

Bringué, M., and A. Rochon (2012), Late Holocene paleoceanography and climate variability over the Mackenzie Slope (Beaufort Sea, Canadian Arctic), *Mar. Geol.*, *291–294*, 83–96, doi:10.1016/j.margeo.2011.11.004.

Brumsack, H. J. (1989), Geochemistry of recent TOC-rich sediments from the Gulf of California and the Black Sea, *Geol. Rundsch.*, *78*, 851–882, doi:10.1007/BF01829327.

Burdige, D. J. (1993), The biogeochemistry of manganese and iron reduction in marine sediments, *Earth Sci. Rev.*, *35*, 249–284, doi:10.1016/0012-8252(93)90040-E.

Calvert, S. E., and T. F. Pedersen (2007), Elemental proxies for palaeoclimatic and palaeoceanographic variability in marine sediments: Interpretation and application, in *Proxies in Late Cenozoic Paleoceanography*, edited by C. Hillaire-Marcel and A. D. Vernal, pp. 567644, Elsevier, Amsterdam.

Carmack, E. C., and R. W. Macdonald (2002), Oceanography of the Canadian shelf of the Beaufort Sea: A setting for marine life, *Arctic*, *55*, 29–45, doi:10.1126/science.100.2596.291.

Carson, M. A., J. N. Jasper, and P. M. Conly (1998), Magnitude and sources of sediment input to the Mackenzie Delta, Northwest Territories, 1974-94, *Arctic*, *51*, 116–124.

Childs, C. (2004), Interpolating surfaces in ArcGIS spatial analyst, *ArcUser*, *27*, 32–35. [Available at http://www.esri.com/news/arcuser/0704/files/interpolating.pdf.]

Darby, D., J. Bischof, G. Cutter, A. Vernal, C. Hillaire-Marcel, G. Dwyer, J. McManus, L. Osterman, L. Polyak, and R. Poore (2001), New record shows pronounced changes in Arctic Ocean circulation and climate, *Eos Trans. AGU*, *82*, 601–607.

Darby, D. A. (2003), Sources of sediment found in sea ice from the western Arctic Ocean, new insights into processes of entrainment and drift patterns, *J. Geophys. Res.*, *108*(C8), 3257, doi:10.1029/2002JC001350.

Darby, D. A., L. Polyak, and H. A. Bauch (2006), Past glacial and interglacial conditions in the Arctic Ocean and marginal seas: A review, *Prog. Oceanogr.*, *71*, 129–144, doi:10.1016/j.pocean.2006.09.009.

Darby, D. A., W. B. Myers, M. Jakobsson, and I. Rigor (2011), Modern dirty sea ice characteristics and sources: The role of anchor ice, *J. Geophys. Res.*, *116*, C09008, doi:10.1029/2010JC006675.

Darby, D. A, J. D. Ortiz, C. E. Grosch, and S. P. Lund (2012), 1,500-year cycle in the Arctic Oscillation identified in Holocene Arctic sea-ice drift, *Nat. Geosci.*, *5*, 897–900, doi:10.1038/ngeo1629.

Davidson, S., K. Lank, and S. De Margerie (1988), *Sediment Transport in the Mackenzie River Plume, Geol. Surv. Canada, Open File*, *92*, 92 pp. [Available at http://ftp.geogratis.gc.ca/pub/nrcan_rncan/publications/ess_sst/131/131307/of_2303.pdf.]

Day, R., M. Fuller, and V. A. Schmidt (1977), Hysteresis properties of titanomagnetites: Grain-size and compositional dependence, *Phys. Earth Planet. Int.*, *13*, 260–267.

Dietze, E., K. Hartmann, B. Diekmann, J. IJmker, F. Lehmkuhl, S. Opitz, G. Stauch, Wünnemann, B., and A. Borchers (2012), An end-member algorithm for deciphering modern detrital processes from lake sediments of Lake Donggi Cona, NE Tibetan Plateau, China, *Sediment. Geol.*, *243-244*, 169–180, doi:10.1016/j.sedgeo.2011.09.014.

Dunlop, D. J. (2002), Theory and application of the Day plot (Mrs/Ms versus Hcr/Hc) 1. Theoretical curves and tests using titanomagnetite data, *J. Geophys. Res.*, *107*(B3), 2056, doi:10.1029/2001JB000486.

Dunlop, D. J., and Ö. Özdemir (1997), *Rock Magnetism: Fundamentals and Frontiers*, Cambridge Univ. Press, Cambridge, U. K.

Durantou, L., A. Rochon, D. Ledu, Massé, G., S. Schmidt, and M. Babin (2012), Quantitative reconstruction of sea-surface conditions over the last 150 yr in the Beaufort Sea based on dinoflagellate cyst assemblages: The role of large-scale atmospheric circulation patterns, *Biogeosciences*, *9*, 5391–5406, doi:10.5194/bg-9-5391-2012.

Fagel, N., C. Not, J. Gueibe, N. Mattielli, and E. Bazhenova (2014), Late Quaternary evolution of sediment provenances in the Central Arctic Ocean: Mineral assemblage, trace element composition and Nd and Pb isotope fingerprints of detrital fraction from the Northern Mendeleev Ridge, *Quat. Sci. Rev.*, *92*, 140–154, doi:10.1016/j.quascirev.2013.12.011.

Forest, A., M. Sampei, R. Makabe, H. Sasaki, D. G. Barber, Y. Gratton, P. Wassmann, and L. Fortier (2008), The annual cycle of particulate organic carbon export in Franklin Bay (Canadian Arctic): Environmental control and food web implications, *J. Geophys. Res.*, *113*, C03S05, doi:10.1029/2007JC004262.

Galley, R. J., E. Key, D. G. Barber, B. J. Hwang, and J. K. Ehn (2008), Spatial and temporal variability of sea ice in the southern Beaufort Sea and Amundsen Gulf: 1980–2004, *J. Geophys. Res.*, *113*, C05S95, doi:10.1029/2007JC004553.

Giovando,L. F., and R. H. Herlinveaux (1981), A discussion of factors influencing dispersion of pollutants in the Beaufort Sea, *Pac. Mar. Sci. Rep.*, *81–4*, 198 pp.

Grunsky, E. C., L. J. Drew, L. G. Woodruff, P. W. B. Friske, and D. M. Sutphin (2013), Statistical variability of the geochemistry and mineralogy of soils in the Maritime Provinces of Canada and part of the Northeast United States, *Geochemistry Explor. Environ. Anal.*, *13*(4), 249.

Harrison, J. C., et al. (2008), Geological Map of the Arctic, *Geol. Surv. Canada Open File, 5816*, 5 sheets, doi:10.4095/225705.

Harrison, J. C., et al. (2011), Geological map of the Arctic, *Geol. Surv. of Can. Open File, 5816*, doi:10.4095/287868.

Hill, P. R., S. M. Blasco, J. R. Harper, D. B. Fissel, D. Bornhold, T. Atlantic, G. Centre, and B. R. Pelletier (1991), Sedimentation on the Canadian Beaufort Shelf, *Cont. Shelf Res.*, *11*, 821–842, doi:10.1016/0278-4343(91)90081-G.

Hill, P. R., A. Héquette, and M.-H. Ruz (1993), Holocene sea-level history of the Canadian Beaufort shelf, *Can. J. Earth Sci.*, *30*, 103–108, doi:10.1139/e93-009.

Hill, P. R., C. P. Lewis, S. Desmarais, V. Kauppaymuthoo, and H. Rais (2001), The Mackenzie Delta: Sedimentary processes and facies of a high-latitude, fine-grained delta, *Sedimentology*, *48*, 1047–1078, doi:10.1046/j.1365-3091.2001.00408.x.

Holmes, R. M., J. W. McClelland, B. J. Peterson, I. A. Shiklomanov, A. I. Shiklomanov, A. V. Zhulidov, V. V. Gordeev, and N. N. Bobrovitskaya (2002), A circumpolar perspective on fluvial sediment flux to the Arctic ocean, *Global Biogeochem. Cycles*, *16*(4), 1098, doi:10.1029/2001GB001849.

Kaufman, L., and P. J. Rousseeuw (2009), *Finding Groups in Data: An Introduction to Cluster Analysis Wiley Ser. Probab. Stat.*, 356 pp., John Wiley, Hoboken, N. J., doi:10.1002/9780470316801.

Kwok, R., G. F. Cunningham, M. Wensnahan, I. Rigor, H. J. Zwally, and D. Yi (2009), Thinning and volume loss of the Arctic Ocean sea ice cover: 2003–2008, *J. Geophys. Res.*, *114*, C07005, doi:10.1029/2009JC005312.

Lammers, R. B., A. I. Shiklomanov, C. J. Vörösmarty, B. M. Fekete, and B. J. Peterson (2001), Assessment of contemporary Arctic river runoff based on observational discharge records, *J. Geophys. Res.*, *106*, 3321–3334, doi:10.1029/2000JD900444.

Lanos, R. (2009), Circulation régionale, masses d'eau, cycles d'évolution et transports entre la mer de Beaufort et le golfe d'Amundsen. PhD thesis. Québec, Université du Québec, Institut national de la recherche scientifique, Doctorat en sciences de l'eau, 274 pp. [Available at http://espace.inrs.ca/id/eprint/480.]

Linsen, D., S. H. I. Xuefa, L. I. U. Yanguang, F. Xisheng, C. Zhihua, W. Chunjuan, Z. O. U. Jianjun, and H. Yuanhui (2014), Mineralogical study of surface sediments in the western Arctic Ocean and their implications for material sources, *Adv. Polar Sci.*, *25*, 192–203, doi:10.13679/j.advps.2014.3.00192.

Lisé-Pronovost, A., G. St-Onge, S. Brachfeld, F. Barletta, and D. Darby (2009), Paleomagnetic constraints on the Holocene stratigraphy of the Arctic Alaskan margin, *Global Planet. Change*, *68*, 85–99, doi:10.1016/j.gloplacha.2009.03.015.
Lu, Y., X. Sun, Z. Lin, and H. Lu (2014), Authigenic carbonate mineralogy, South China Sea and its relationship with cold seep activity, *Acta Geol. Sin*. [English ed.], *88*, 1473–1474.
Macdonald, R. W., and C. Gobeil (2012), Manganese sources and sinks in the Arctic Ocean with reference to periodic enrichments in basin sediments, *Aquat. Geochem.*, *18*, 565–591, doi:10.1007/s10498-011-9149-9.
Macdonald, R. W., D. W. Paton, E. C. Carmack, and A. Omstedt (1995), The freshwater budget and under-ice spreading of Mackenzie River water in the Canadian Beaufort Sea based on salinity and 18O/16O measurements in water and ice, *J. Geophys. Res.*, *100*, 895–919, doi: 10.1029/94JC02700.
Macdonald, R. W., S. M. Solomon, R. E. Cranston, H. E. Welch, M. B. Yunker, and C. Gobeil (1998), A sediment and organic carbon budget for the Canadian Beaufort Shelf, *Mar. Geol.*, *144*, 255–273, doi:10.1016/S0025-3227(97)00106-0.
Macdonald, R. W., T. Harner, and J. Fyfe (2005), Recent climate change in the Arctic and its impact on contaminant pathways and interpretation of temporal trend data, *Sci. Total Environ.*, *342*, 5–86, doi:10.1016/j.scitotenv.2004.12.059.
MacNeil, M. R., and J. R. Garrett (1975), Open water surface currents, *Beaufort Sea Tech. Rep.*, *17*, 113 pp.
Maechler, M., P. Rousseeuw, A. Struyf, M. Hubert, and K. Hornik (2015), cluster: Cluster Analysis Basics and Extensions, 2015, R package. [Available at http://cran.r-project.org/web/packages/cluster/.]
Magen, C. (2007), Origin, sedimentation and diagenesis of organic matter in coastal sediments of the southern Beaufort Sea region, Canadian Arctic, PhD thesis, 130 pp., McGill Univ., Montreal.
Magen, C., G. Chaillou, S. A. Crowe, A. Mucci, Sundby. B., A. G. Gao, R. Makabe, and H. Sasaki (2010), Origin and fate of particulate organic matter in the southern Beaufort Sea: Amundsen Gulf region, Canadian Arctic, *Estuarine Coastal Shelf Sci.*, *86*(1), 31–41.
Magen, C., A. Mucci, and B. Sundby (2011), Reduction rates of sedimentary Mn and Fe Oxides: An incubation experiment with arctic ocean sediments, *Aquat. Geochem.*, *17*, 629–643, doi:10.1007/s10498-010-9117-9.
Meinhardt, A. K., C. März, R. Stein, and H. J. Brumsack (2014),. Regional variations in sediment geochemistry on a transect across the Mendeleev Ridge (Arctic Ocean), *Chem. Geol.*, *369*, 1–11, doi:10.1016/j.chemgeo.2014.01.011.
Millot, R., J. Gaillardet, B. Dupré, and C. J. Allégre (2003), Northern latitude chemical weathering rates: Clues from the Mackenzie River Basin, Canada, *Geochim. Cosmochim. Acta*, *67*, 1305–1329, doi:10.1016/S0016-7037(02)01207-3.
Montero-Serrano, J. C., V. Bout-Roumazeilles, N. Tribovillard, T. Sionneau, A. Riboulleau, A. Bory, and B. Flower (2009), Sedimentary evidence of deglacial megafloods in the northern Gulf of Mexico (Pigmy Basin), *Quat. Sci. Rev.*, *28*, 3333–3347.
Montero-Serrano, J. C., V. Bout-Roumazeilles, T. Sionneau, N. Tribovillard, A. Bory, B. P. Flower, A. Riboulleau, P. Martinez, and I. Billy (2010a), Changes in precipitation regimes over North America during the Holocene as recorded by mineralogy and geochemistry of Gulf of Mexico sediments, *Global Planet. Change*, *74*, 132–143.
Montero-Serrano, J. C., J. Palarea-Albaladejo, J. A. Martin-Fernandez, M. Martinez-Santana, and J. V. Gutierrez-Martin (2010b), Sedimentary chemofacies characterization by means of multivariate analysis, *Sediment. Geol.*, *228*, 218–228, doi:10.1016/j.sedgeo.2010.04.013.
Montero-Serrano, J. C., K. B. Föllmi, T. Adatte, J. E. Spangenberg, N. Tribovillard, A. Fantasia, and G. Suan (2015), Continental weathering and redox conditions during the early Toarcian Oceanic Anoxic Event in the northwestern Tethys: Insight from the Posidonia Shale section in the Swiss Jura Mountains, *Palaeogeogr. Palaeoclimatol. Palaeoecol.*, *429*, 83–99.
Moore, T. S., R. W. Murray, A. C. Kurtz, and D. P. Schrag (2004), Anaerobic methane oxidation and the formation of dolomite, *Earth Planet. Sci. Lett.*, *229*, 141–154, doi:10.1016/j.epsl.2004.10.015.
Mucci, A., B. Lansard, L. A. Miller, and T. N. Papakyriakou (2010), CO2 fluxes across the air-sea interface in the southeastern Beaufort Sea: Ice-free period, *J. Geophys. Res.*, *115*, C04003, doi:10.1029/2009JC005330.
Naidu, A. S., and T. C. Mowatt (1983), Sources and dispersal patterns of clay minerals in surface sediments from the continental-shelf areas off Alaska, *Geol. Soc. Am. Bull.*, *94*, 841–854.
Naidu, A. S., D. C. Burrell, and D. H. Wood (1971), Clay mineral composition and geologic significance of some beaufort sea sediments, *J. Sediment. Petrol.*, *41*, 691–694, doi:10.1306/74D72329-2B21-11D7-8648000102C1865D.
Naidu, A. S., J. S. Creager, and T. C. Mowatt (1982), Clay mineral dispersal patterns in the north Bering and Chukchi Seas, *Mar. Geol.*, *47*, 1–15, doi:10.1016/0025-3227(82)90016-0.
O'Brien, M. C., R. W. Macdonald, H. Melling, and K. Iseki (2006), Particle fluxes and geochemistry on the Canadian Beaufort Shelf: Implications for sediment transport and deposition, *Cont. Shelf Res.*, *26*, 41–81, doi:10.1016/j.csr.2005.09.007.
Oksanen, J., F. G. Blanchet, R. Kindt, P. Legendre, P. R. Minchin, O'R. B. Hara, G. L. Simpson, P. Solymos, M. H. H. Stevens, and H. Wagner (2015), vegan: Community Ecology Package. R package version 2.3-2. [Available at http://cran.r-project.org/web/packages/vegan/index.html.]
Ortiz, J. D., L. Polyak, J. M. Grebmeier, D. Darby, D. D. Eberl, S. Naidu, and D. Nof (2009), Provenance of Holocene sediment on the Chukchi-Alaskan margin based on combined diffuse spectral reflectance and quantitative X-Ray Diffraction analysis, *Global Planet. Change*, *68*, 73–84, doi:10.1016/j.gloplacha.2009.03.020.
Overland, J. E., J. M. Adams, and N. A. Bond (1999), Decadal variability of the Aleutian Low and its relation to high-latitude circulation, *J. Clim.*, *12*, 1542–1548.
Padgham, W. A., and W. K. Fyson (1992), The slave province: A distinct Archean craton, *Can. J. Earth Sci.*, *29*, 2072–2086, doi:10.1139/e92-165.
Pancost, R. D., I. Bouloubassi, G. Aloisi, J. S. S. Damsté, and the Medinaut Shipboard Scientific Party (2001), Three series of non-isoprenoidal dialkyl glycerol diethers in cold-seep carbonate crusts, *Org. Geochem.*, *32*, 695–707, doi:10.1016/S0146-6380(01)00015-8.
Paull, C.K., et al. (2015), Active mud volcanoes on the continental slope of the Canadian Beaufort Sea, *Geochem. Geophys. Geosyst.*, *16*, 3160–3181, doi:10.1002/2015GC005928.
Paull, C. K., W. Ussler, S. R. Dallimore, S. M. Blasco, T. D. Lorenson, H. Melling, B. E. Medioli, F. M. Nixon, and F. A. McLaughlin (2007), Origin of pingo-like features on the Beaufort Sea shelf and their possible relationship to decomposing methane gas hydrates, *Geophys. Res. Lett.*, *34*, L01603, doi:10.1029/2006GL027977.
Pelletier, B. R. (1975), Sediment dispersal in the southern Beaufort Sea. Beaufort Sea Project, *Tech. Rep. 25a*, 80 pp., Dep. of the Environ., Victoria, B. C.
Pickart, R. S. (2004), Shelfbreak circulation in the Alaskan Beaufort Sea: Mean structure and variability, *J. Geophys. Res.*, *109*, C04024, doi: 10.1029/2003JC001912.
Reimann, C., P. Filzmoser, R. Garrett, and R. Dutter (2008), *Statistical Data Analysis Explained: Applied Environmental Statistics With R*, 343 pp., John Wiley, Chichester, U. K.
Reimnitz, E., J. R. Clayton, E. W. Kempema, J. R. Payne, and W. S. Weber (1993), Interaction of rising frazil with suspended particles: Tank experiments with applications to nature, *Cold Reg. Sci. Technol.*, *21*, 117–135, doi:10.1016/0165-232X(93)90002-P.

Richerol, T., A. Rochon, S. Blasco, D. B. Scott, T. M. Schell, and R. J. Bennett (2008a), Evolution of paleo sea-surface conditions over the last 600 years in the Mackenzie Trough, Beaufort Sea (Canada), *Mar. Micropaleontol.*, *68*, 6–20, doi:10.1016/j.marmicro.2008.03.003.

Richerol, T., A. Rochon, S. Blasco, D. B. Scott, T. M. Schell, and R. J. Bennett (2008b), Distribution of dinoflagellate cysts in surface sediments of the Mackenzie Shelf and Amundsen Gulf, Beaufort Sea (Canada), *J. Mar. Syst.*, *74*, 825–839, doi:10.1016/j.jmarsys.2007.11.003.

Saint-Ange, F., P. Kuus, S. Blasco, D. J. W. Piper, J. H. Clarke, and K. MacKillop (2014), Multiple failure styles related to shallow gas and fluid venting, upper slope Canadian Beaufort Sea, northern Canada, *Mar. Geol.*, *355*, 136–149, doi:10.1016/j.margeo.2014.05.014.

Schell, T. M., T. J. Moss, D. B. Scott, and A. Rochon (2008), Paleo-sea ice conditions of the Amundsen Gulf, Canadian Arctic Archipelago: Implications from the foraminiferal record of the last 200 years, *J. Geophys. Res.*, *113*, C03S02, doi:10.1029/2007JC004202.

Schoster, F., M. Behrends, R. Muller, R. Stein, and M. Washner (2000), Modern river discharge and pathways of supplied material in the Eurasian Arctic Ocean: Evidence from mineral assemblagesand major and minor element distribution, *Int. J. Earth Sci.*, *89*, 486–495, doi:10.1007/s005310000120.

Scott, D. B., T. Schell, A. Rochon, and S. Blasco (2008), Benthic foraminifera in the surface sediments of the Beaufort Shelf and slope, Beaufort Sea, Canada: Applications and implications for past sea-ice conditions, *J. Mar. Syst.*, *74*, 840–863, doi:10.1016/j.jmarsys.2008.01.008.

Scott, D. B., T. Schell, G. St-Onge, A. Rochon, and S. Blasco (2009), Foraminiferal assemblage changes over the last 15,000 years on the Mackenzie-Beaufort Sea Slope and Amundsen Gulf, Canada: Implications for past sea ice conditions, *Paleoceanography*, *24*, PA2219, doi:10.1029/2007PA001575.

Shearer, J. M., R. F. Macnab, B. R. Pelletier, and T. B. Smith (1971), Submarine Pingos in the Beaufort Sea, *Science*, *174*, 816–818.

Simon, Q., G. St-Onge, and C. Hillaire-Marcel (2012), Late Quaternary chronostratigraphic framework of deep Baffin Bay glaciomarine sediments from high-resolution paleomagnetic data, *Geochem. Geophys. Geosyst.*, *13*, Q0AO03, doi:10.1029/2012GC004272.

Stein, R. (2008), Arctic Ocean sediments: Processes, proxies, and paleoenvironment, in *Developments in Marine Geology*, vol. 2, 592 pp., Elsevier, Amsterdam.

Stokes, C. R., C. D. Clark, and C. M. Winsborrow (2006), Subglacial bedform evidence for a major palaeo-ice stream and its retreat phases in Amundsen Gulf, Canadian Arctic Archipelago, *J. Quat. Sci.*, *21*, 399–412, doi:10.1002/jqs.991.

Stoner, J. S., and G. St-Onge (2007), Chapter three magnetic stratigraphy in paleoceanography: Reversals, excursions, paleointensity, and secular variation, *Dev. Mar. Geol.*, *1*, 99–138, doi:10.1016/S1572-5480(07)01008-1.

Tremblay, J.-É., P. Raimbault, N. Garcia, B. Lansard, M. Babin, and J. Gagnon (2014), Impact of river discharge, upwelling and vertical mixing on the nutrient loading and productivity of the Canadian Beaufort Shelf, *Biogeosciences*, *11*, 4853–4868, doi:10.5194/bg-11-4853-2014.

Tribovillard, N., T. J. Algeo, T. Lyons, and A. Riboulleau (2006), Trace metals as paleoredox and paleoproductivity proxies: An update, *Chem. Geol.*, *232*, 12–32.

van den Boogaart, K. G., and R. Tolosana-Delgado (2008), "compositions": A unified R package to analyze compositional data, *Comput. Geosci.*, *34*, 320–338, doi:10.1016/j.cageo.2006.11.017.

Viscosi-Shirley, C., K. Mammone, N. Pisias, and J. Dymond (2003), Clay mineralogy and multi-element chemistry of surface sediments on the Siberian-Arctic shelf: Implications for sediment provenance and grain size sorting, *Cont. Shelf Res.*, *23*, 1175–1200, doi:10.1016/S0278-4343(03)00091-8.

Vogt, C. (1997), Regional and temporal variations of mineral assemblages in Arctic Ocean sediments as climatic indicator during glacial/interglacial changes, *Rep. Polar Res.*, *251*, 309.

von Eynatten, H., C. Barcelo-Vidal, and V. Pawlowsky-Glahn (2003), Composition and discrimination of sandstones: A statistical evaluation of different analytical methods, *J. Sediment. Res.*, *73*, 47–57, doi:10.1306/070102730047.

von Eynatten, H., R. Tolosana-Delgado, V. Karius, K. Bachmann, and L. Caracciolo (2016), Sediment generation in humid Mediterranean setting: Grain-size and source-rock control on sediment geochemistry and mineralogy (Sila Massif, Calabria), *Sediment. Geol.*, *336*, 68–80, doi:10.1016/j.sedgeo.2015.10.008.

Vonk, J. E., L. Giosan, J. Blusztajn, D. Montlucon, E. G. Pannatier, C. McIntyre, L. Wacker, R. W. Macdonald, M. B. Yunker, and T. I. Eglinton (2015), Spatial variations in geochemical characteristics of the modern Mackenzie Delta sedimentary system, *Geochim. Cosmochim. Acta*, *171*, 100–120, doi:10.1016/j.gca.2015.08.005.

Wagner, A., G. Lohmann, and M. Prange (2011), Arctic river discharge trends since 7ka BP, *Global Planet. Change*, *79*, 48–60, doi:10.1016/j.gloplacha.2011.07.006.

Wedepohl, K. H. (1991), The composition of the upper earth's crust and the natural cycles of selected metals: Metals in natural raw materials. Natural resources, *in Metals and Their Compounds in the Environment*, edited by E. Merian, pp. 3–17, VCH, Weinheim.

Weltje, G. J. (1997), End-member modeling of compositional data: Numerical-statistical algorithms for solving the explicit mixing problem, *Math. Geol.*, *29*, 503–549, doi:10.1007/BF02775085.

White, A. F., T. D. Bullen, M. S. Schulz, A. E. Blum, T. G. Huntington, and N. E. Peters (2001), Differential rates of feldspar weathering in granitic regoliths, *Geochim. Cosmochim. Acta*, *65*, 847–869, doi:10.1016/S0016-7037(00)00577-9.

Yang, L. U., S. U. N. Xiaoming, L. I. N. Zhiyong, and L. U. Hongfeng (2014), Authigenic carbonate mineralogy, South China Sea and its relationship with cold seep activity, *88*.

Young, R. A. (1993), *The Rietveld Method. International Union of Crystallography Monographs on Crystallography 5 [Chester, England]*, 308 p., Int, Union of Crystallogr, Oxford Univ. Press, Oxford, New York.